CHALMERS
UNIVERSITY OF TECHNOLOGY

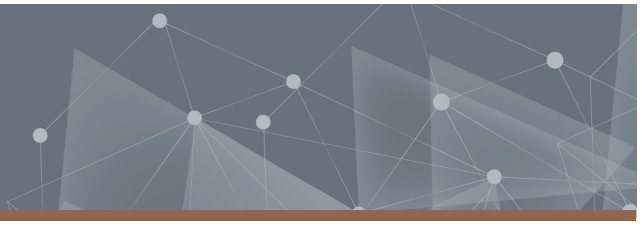

How can perceived vertical choppiness in the driver seat be improved in an electric vehicle

Master's thesis in Mobility Engineering

KUMARESH KUNAL

DEPARTMENT OF MECHANICS AND MARITIME SCIENCES (M2)

CHALMERS UNIVERSITY OF TECHNOLOGY
Gothenburg, Sweden 2023
www.chalmers.se

Master's thesis 2023

How can perceived vertical choppiness in the driver seat be improved in an electric vehicle

KUMARESH KUNAL

Department of Mechanics and Maritime Sciences (M2)
Division of Vehicle Engineering and Autonomous Systems
Chalmers University of Technology
Gothenburg, Sweden 2023

Supervisors:
Bosse Krüger
Attribute Leader Ride Comfort
Chassis Concept Attributes (91640)
Volvo Cars

Erik Wendeberg
CAE Engineer
Chassis Concept Attributes (91640)
Volvo Cars

Examiner:
Bengt Jacobson
Professor and Group leader-Vehicle Dynamics
Department of Mechanics and Maritime Sciences
Chalmers University of Technology

Master's Thesis 2023
Department of Mechanics and Maritime Sciences (M2)
Division of Vehicle Engineering and Autonomous Systems
Chalmers University of Technology
SE-412 96 Gothenburg
Telephone +46 31 772 1000

Cover:

Typeset in LaTeX
Printed by Chalmers Reproservice
Gothenburg, Sweden 2023

Abstract

It's essential to understand both the positive and negative implications of the automobile industry's transition from traditional internal combustion engine (ICE) vehicles to electric vehicles (EVs). One such negative impact is the vertical choppiness levels in an EV. Choppiness, considered a part of ride comfort, is defined as road-induced uneven pitch and bounce motions of the vehicle. It can be felt between the frequency ranges of 3 and 8 Hz. Choppiness is more predominant when the vehicle is driven over an irregular or rough surface. As humans have the lowest tolerance for vibrations between 3 and 8 Hz, high degrees of choppiness impact the abdomen region as well as the voice of the occupants. The ICE, together with its engine mounts, acts as a heavy mass damper, reducing vibration input to the driver and occupants' seats at 3-8Hz, whereas the electric motor is not as heavy and has less potential to reduce choppiness, hence increasing choppiness in a BEV. It is crucial to think about the impact of choppiness because ride comfort is one of the most important elements a customer evaluates when buying a new vehicle.

This thesis focuses on finding low cost solutions by examining the interaction of the driver in the seat with the suspension to reduce the choppiness without having a negative impact on the shake vibration region (8-20Hz). Air suspensions are one way to reduce the choppiness, but they cannot be used in every vehicle due to their high cost. The thesis proposal attempts to validate the potential of altering the seat characteristics, i.e., the seat spring and damping, in order to lower the levels of choppiness perceived in the driver's seat of a BEV, using CAE ride models. The effects of the driver's vertical seat bounce frequency on choppiness were investigated using these ride models, as well as design modifications that have an impact on choppiness levels. The results obtained from these models were also validated by comparing them with tests done on the actual vehicle on the shake rig. When these models were run on different virtual roads, the corresponding responses were recorded and used for further calculation of RMS acceleration values of the seat, which was the cost function chosen to quantify the choppiness levels of the ride models in accordance with the international standards in place for the effect of environmental vibration on operator health, efficiency, and comfort (ISO 2631).

Keywords: choppiness, ride comfort, CAE ride models, seat parameters, validation, BEV, ICE, ISO 2631, efficiency, RMS acceleration .

Acknowledgements

I would like to thank my supervisors, Bosse Krüger and Erik Wendeberg, as well as the Volvo Cars Corporation Chassis Concept Attributes team, for their unwavering support and assistance throughout the duration of this thesis project. Their advice and expertise were instrumental not only in broadening my technical skills but also in ensuring the successful completion of my research. I also want to take this opportunity to thank my team manager, Kristofer Weiner, for his assistance in making the necessary arrangements throughout the project. His assistance was critical to the thesis's smooth progress.

Furthermore, I would like to thank Biki Sarmah and Vishwas Sharma from Volvo Cars Corporation's Chassis Concept Attributes team for their exceptional coordination and assistance. Their collaboration and support were significant in overcoming obstacles and achieving my thesis objectives. Last but not least, I would like to express my heartfelt gratitude to Bengt Jacobson, Professor and Group Leader-Vehicle Dynamics at Chalmers University of Technology, for serving as our examiner and providing continuous assistance and valuable feedback throughout the thesis work. His expertise and advice were invaluable in shaping the thesis's direction.

Kunal Kumaresh,
Gothenburg, 2023

List of Acronyms

Below is the list of acronyms that have been used throughout this thesis listed in alphabetical order:

BEV	Battery Electric Vehicle
BMI	Body Mass Index
CAE	Computer Aided Engineering
DOF	Degree of Freedom
EFAD	Electric Front Axle Drive
ERAD	Electric Rear Axle Drive
EV	Electric Vehicle
ICE	Internal Combustion Engine
ISO	International organisation for standardization
PSD	Power Spectral Density
RMS	Root Mean Square
SUV	Sports Utility Vehicle
VCC	Volvo Cars Corporation
VDV	Vibration Dose Value

Contents

List of Figures

List of Tables

1 Introduction

When buying a vehicle, one of the crucial factors to consider is ride comfort. The more comfortable the ride, the fewer problems the driver and passengers endure thereby increasing driver performance, improving safety and human health as well (Hemanth and Joshua[4]). Therefore, it is an important design criteria when developing new vehicles.

1.1 Background

Automobiles travel at high speeds on roads that are not always smooth causing the occupants to experience a broad spectrum of vibration. Therefore, vertical dynamics should be looked into in order to learn about the human perception of vibrations (ride comfort) when the vehicle is driven on irregular surfaces.

A vehicle's complete comfort cannot be defined in a single way because several factors influence vehicle comfort. They are classified into three groups: ambient, dynamic, and ergonomic. Ambient elements include air temperature, air quality, sound, and so on, whereas ergonomic aspects include seatbelts, seat architecture, visibility, and so on, and dynamic factors include vibrations, impact, ride motion, and acceleration (X. Wang et al., 2020[1]).

The thesis focuses on the dynamic factors that affect the ride comfort of vehicles. The sensation or feeling of a passenger in the environment of a moving vehicle is addressed by ride comfort. The comfort that vehicle occupants experience from stationary oscillations when the vehicle travels over a road with a certain vertical irregularity at a certain speed is referred to as ride comfort.

The ride comfort measure is defined as including at least the driver seat, along with the driver's vertical acceleration amplitudes. Ride comfort is usually divided into two categories, they are primary ride and secondary ride. Primary ride is generally associated with rigid body movements in the frequency range of 0-3 Hz whereas secondary ride is associated with frequencies in the range of (3-25 Hz).

Ride comfort issues are primarily caused by vibrations in the seats, which are transmitted from the vehicle body. The vibrations can be caused by a variety of factors such as road surface irregularities, vibration from the power source and driveline, and tire/wheel assembly imbalances (non-uniformities). Road surface irregularities, such as random variations in surface profile elevation, potholes, and so on, are major sources of vibration that excite the vibration of the vehicle via the suspension system and tire/wheel assembly.

Choppiness is an aspect of ride comfort; it is most commonly felt in the secondary ride frequency ranges of 3-8Hz, and is defined as road induced (continuous), irregular pitch and bounce motions of the vehicle above the primary ride frequency. When driving on smooth roads, choppiness is not an issue; however with more road unevenness, choppiness becomes more important to mitigate. High levels of choppiness

distort the voice of occupants when speaking or singing in the car, also it makes car feel cheaper and less refined.

When investigating the human response to vibrations and shocks, both mechanical and psychological effects should be considered. The goal is to keep shocks from affecting the human body, so understanding the human response to vibration characteristics is critical. In general, passenger ride comfort (or discomfort) boundaries are difficult to determine because of the variations in individual sensitivity to vibration.

1.2 Problem Statement

Changing the powertrain from a conventional ICE to an electric powertrain powered by electric motors has both positive and negative implications for ride comfort. The aim is to look into low-cost solutions to mitigate the negative effects. Choppiness is one such negative impact that this thesis work aims to reduce.

Increased level of vertical vibrations in 3-8 Hz region leads to more pronounced choppiness, perceived by driver and front passenger. The ICE on its engine mounts works as a heavy mass damper which heavily reduces vibration input to seats in the frequency range of 3-8 Hz. Electric powertrains have lower mass and by that less potential to reduce choppiness there by increasing the choppiness in an electric vehicle.

The choppiness can be reduced by using air suspension with low primary ride frequencies; however, because air suspensions are expensive, they cannot be used on all vehicles. One challenge is to broaden traditional vehicle dynamics studies to include the interaction of the driver in the seat with the suspension. By carrying out this thesis, it is possible to investigate the potential in seat suspension and find cost-effective ways to reduce choppiness without having negative effects on shake (8-20Hz)vibration.

1.3 Aims and Tasks

The choppiness increases when a combustion engine (ICE) is replaced by an electric motor. The aim of this thesis is to reduce choppiness in an electric vehicle and to identify and quantify actions that affect choppiness. To do this, the following tasks were performed :

- CAE ride model was built in MATLAB and Simulink.
- How the driver's vertical bounce frequency on the seat effects choppiness, and how vibrations ranging from 8 to 20Hz affect the driver/passenger was studied using these ride models.
- Many parts were included in the model, such as road, wheel suspension, pow-

ertrain suspension, vehicle body motion and seats were modelled.

- After identifying design variations that affect choppiness, the effect was verified using the models.

- The CAE ride models were validated by performing similar tests with test person on the seat in the vehicle on the shake rig

- The seat parameters were varied in order to see the effect on choppiness and understand the scope of making a better seat to reduce the choppiness and improve the overall ride comfort.

1.4 Outline of Work

The thesis report consists of the following sections:

- **Chapter 1:** Provides an introduction and understanding of the problem statement being solved in thesis. Also outlines the scope of thesis work.

- **Chapter 2:** Provides the necessary theoretical background of thesis such as the significance of ride comfort,issues faced due to choppiness and the simulation methods used in the thesis work.

- **Chapter 3:** The methodology which was used to solve the problem statement of the thesis where the CAE ride models are explained clearly.

- **Chapter 4:** Provides ways for validating ride models with vehicle test data as well as approaches to understand the influence of wheel hop, powertrain bounce, and other factors on seat vertical frequency.

- **Chapter 5:** The results and findings of the thesis are explained and concluded.

- **Chapter 6:** The potential work that can be done to improve the current thesis work and thereby improve the choppiness in a BEV is discussed.

1.5 Limitations

- Study will be purely vertical, no consideration of load transfer in lateral direction and other lateral and longitudinal effects on the ride model.

- The thesis will focus on only on the secondary ride and especially the choppiness region (3-8Hz). The effect of the varying seat parameters in the shake region will also be studied but the main focus will be on choppiness.

2 Theory

2.1 Vehicle Engineering

The development of complex products, such as vehicles, necessitates the parallel design of numerous subsystems. Front axle suspension, rear axle suspension, driver seat, and propulsion system suspension, for example, all affect choppiness. Many of these, particularly the axle suspensions, have an impact on many other requirements of the entire vehicle, such as driving dynamics. As a result, it is critical to be able to quantify requirements and find a way to break down the overall vehicle requirements to requirements on appropriate subsystems.

2.2 Vehicle Dynamics

The study of vehicle motion, such as the forward movement of the vehicle with respect to the driver inputs, propulsion system outputs, different driving conditions and so on is known as vehicle dynamics. The motions obtained in accelerating, braking, cornering, and ride are responses to forces imposed on the vehicle, and the majority of vehicle dynamics research focuses on understanding how and why these forces act on the vehicle. Vehicle dynamics studies can be divided into three main categories: longitudinal dynamics, lateral dynamics, and vertical dynamics. According to the SAE metric system the vehicle has six degrees of freedom. Translational and rotational movement in the x, y and z axis respectively.

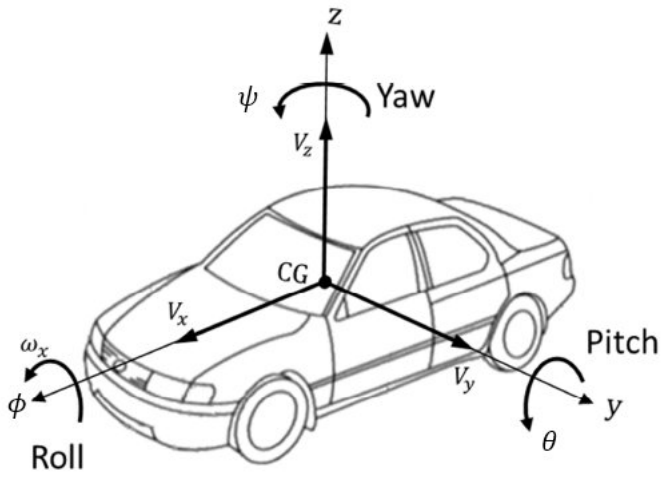

Figure 2.1: Vehicle Co-ordinate System according to SAE standards[11]

2.2.1 Longitudinal Dynamics

The longitudinal dynamics involves the study of the vehicle's performance in the x- direction which is running from the front to rear of the vehicle. This involves the study of the vehicle's acceleration, deceleration, braking and traction control performance.

2.2.2 Lateral Dynamics

The lateral dynamics is the study of the vehicle in the y- direction which is running from the left to the right side of the vehicle. This mainly focuses on the vehicle's stability, steering effects i.e. ability to change direction and cornering performance.

2.2.3 Vertical Dynamics

Vertical Dynamics involves the study of the vehicle performance in the z-direction i.e. the vehicle's vertical direction. Vertical dynamics is primarily concerned with understanding how the suspension system of the vehicle interacts with the other components and absorbs the vibrations hence enhancing ride comfort, fatigue life, and road grip. The thesis work focuses completely on understanding the vertical performance of the vehicle and thus improving ride comfort.

2.3 Ride Comfort

Ride comfort is an important factor to consider for the general public when selecting a vehicle. As a result, it is critical to have a vehicle that provides comfort for passengers, minimizes cargo damage, can reduce driver fatigue on long journeys in uncomfortable vehicles, as well as because road disruption can impact the driver's ability to control the vehicle. A considerable amount of research has been to evaluate the comfort of vehicles. As stated before there are various factors which play apart in affecting the overall comfort of the vehicle.

X. Wang et al.[3], is one of those many researches who has worked on ride comfort and their work indicates that the difference in ride comfort of the conventional ICE vehicles and electric vehicles is yet to be studied and not much research has been done in this field. There is a difference between comfort and discomfort as well as comfort is a physiological and psychological experience, resulting in well being and relaxation of a human being where as discomfort is more of physical experience caused by improper biomechanics and constraints.

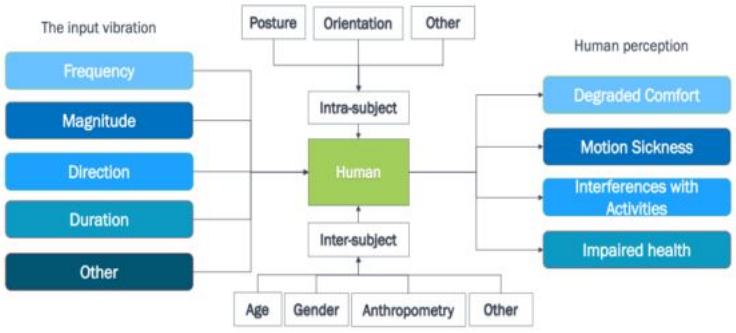

Figure 2.2: Factors influencing overall ride comfort[1]

The vehicle ride behaviour is concerned with vibrations of the vehicle body, which are a function of the body's mass and moment of inertia properties, suspension properties, tyre ride characteristics, aerodynamic forces and irregularities on the road

surface. The vehicle is a dynamic system, but only exhibits vibrations in response to it's excitation inputs. The magnitude and direction of the vibrations placed on the passenger compartment are determined by the vehicle response characteristics, which ultimately impact the passenger's impression of the vehicle. Thus, understanding ride comfort involves study of three main topics:

- Ride excitation source
- Basic mechanics of vehicle vibration response
- Human perception and tolerance of vibrations.

As mentioned before, the thesis focuses on the vehicle dynamic responses and aspects of ride comfort. A simple representation of how ride comfort is estimated is shown in the below figure 2.3.

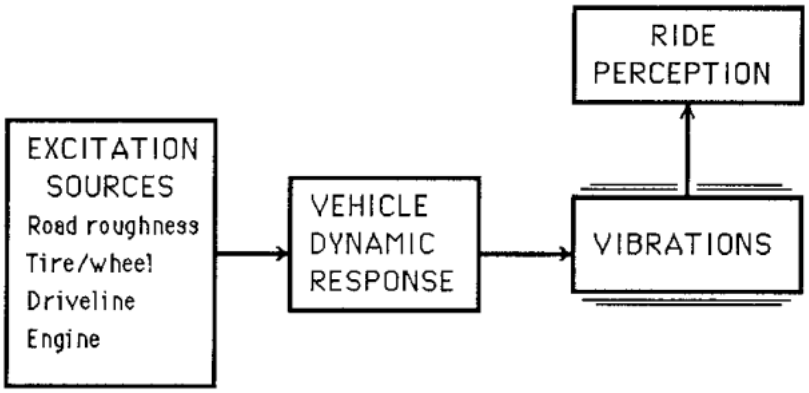

Figure 2.3: Ride comfort analysis done in vehicle dynamics[11]

2.3.1 Seat Comfort

The market competitiveness among automobile manufacturers and customer's perception regarding comfort have increased in recent years. As a result, automobile manufacturers are designing more comfortable and aesthetically pleasing seats in their vehicles. This has been tough due of the difficulty in predicting and analyzing comfort (Hemanth et al.[4]). Vehicle seats are designed in order to provide both static and dynamic comfort to the driver and passenger. De Looze's [5]model explains the main parameters for comfort and discomfort assessment.

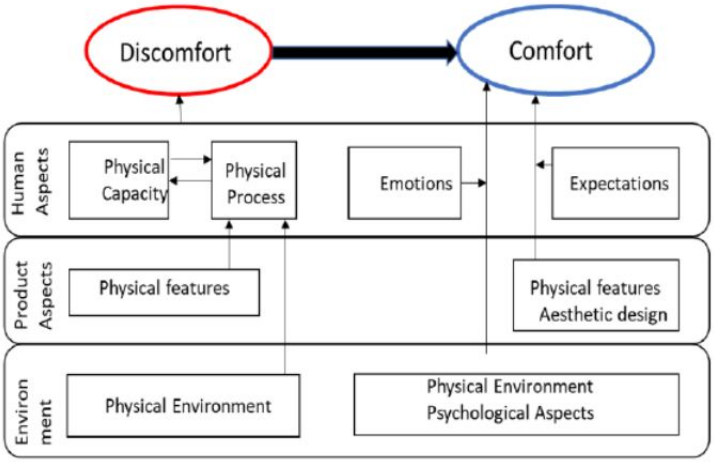

Figure 2.4: De Looze's comfort model[5]

2.4 Ride Excitation Sources

There are multiple sources from which the vehicle can be excited and vibrations can be perceived. They are usually divided into road induced excitation and on board excitation sources. Road generated excitation is caused by varying levels of road roughness, whereas on board excitation is caused by vibrations caused by driveline sources, the prime-mover (engine and/or motor), tire and wheel assemblies.

2.4.1 Road Induced Excitation

The main source of vehicle vibration is excitation caused by road roughness. It is critical to incorporate all aspects such as potholes, speed bumps, uneven road surfaces, and so on while modeling a road. Road roughness is described by the elevation profile along the wheel tracks over which the vehicle passes. Road profiles fit the general category of "broad-band random signals" and hence can be described as the profile itself or it's statistical properties. One of the most useful representation is the power spectral density(PSD) function [11].

The Power Spectral Density (PSD) of a signal is a measure of its power content versus frequency. Typically, a PSD is used to define broadband random signals. The spectral resolution used to digitize the signal normalizes the PSD amplitude. As a result, just like any random process, road surfaces can be expressed using the PSD. The elevation profile measured along the length of a road surface can be divided into a sequence of sine waves with different amplitude and phase connections using the Fourier Transform technique. As a result, the PSD is a plot of amplitude versus frequency.

A road model can incorporate ground properties such as coefficient of friction, damping/elasticity of the ground, and vertical position in general. The independent variable can be one, along an assumed path, or two, x and y in the ground plane. In

this thesis as the area of interest is solely on the vertical behaviour of the vehicle(i.e. vertical dynamics), the road models can be assumed as vertical displacement as a function of path.

The road models can be divided into single frequency road model and multiple frequency road models. (Jacobson et al[10].) For particular roads, such as those made of concrete blocks, a single (spatial) frequency can be a useful approximation to investigate a single wavelength. In addition, the one or single (spatial) frequency road model is useful for understanding the various concepts. A single (spatial) frequency model and a single wave length model are the same thing.

Multiple frequency roads are the ones used to model road roughness and replicate roads present in real world driving scenarios. These are divided into four types :

- Smooth
- Rough
- Very Rough
- Cross Country

2.4.2 Tire/Wheel Assembly

The tire and wheel assembly should be soft and compliant in order to absorb road bumps as part of the isolation system while still running without providing any excitation to the vehicle. In practice, however, flaws in the manufacturing of tires, wheels, hubs, brakes, and other rotating assembly parts can result in non-uniformity of three types, which add to vehicle vibrations. Which are :

- Mass imbalance
- Dimensional Vibration
- Stiffness Variations

All of these non-uniformities interact in the tire/wheel combination, causing changes in the forces and moments at the ground as the vehicle rolls. These are transmitted to the car body via the axles and serve as a source of ride vibrations. The moment fluctuations have little effect on the ride vibrations, but they do have an impact on the steering system vibrations. The forces encountered as a result of these tire shortcomings generate a dynamic imbalance, which primarily affects steering vibrations and has little effect on ride vibrations.

2.4.3 Driveline Excitations

The vibrations that arise from the rotating drivelines are also considered as a ride excitation source. The driveshaft, differential in the drive axle, and axle shafts connecting to the wheels are all part of the driveline. The driveshaft, along with its spline and universal joints, is typically the primary source of driveline excitation, acting as a ride excitation source that causes vehicle vibrations.

2.4.4 Prime Mover Excitation

The principal power source of the vehicle is referred to as the prime mover. The prime mover in a normal ICE vehicle is the engine, while the in a BEV is the motor. The two primary mover excitation sources differ, and the differences in weight and characteristics produce different challenges in the vehicle. Choppiness is one such issue that is more prevalent in a BEV as compared to an ICE car. The prime mover rotates and delivers torque to the driveline, making it a source of ride excitement. As previously stated, the difference in prime movers causes different concerns, and because the engine is heavier, it works as a heavy mass damper, absorbing vibrations input to the vehicle body and therefore the seat.

2.5 Vehicle Dynamic Response

The empirical and analytical approaches are used in vehicle dynamic studies. The empirical technique involves doing many trials and tests on the vehicle in order to understand the various aspects that influence the vehicle's performance. We employ the analytical method as the empirical method can lead to a lot of discrepancies and is time consuming. The analytical approach involves using laws of physics to study the mechanics of the vehicle and also comprehend the numerous aspects that affect the vehicle's performance. The analytical method gives a good head start in the concept phase of a product and can save a lot of time, money and man power[11].

The analytical method comprises of using mathematical models to perform various studies on the vehicle. The method of describing a system using mathematical concepts and language is known as 'mathematical modelling' and the description is called a 'mathematical model'. The main aim of mathematical modelling is to describe all relevant features of the model that enable the derivation of respective equations of motions. Depending on the components the mathematical model can be linear or non linear.

To evaluate the ride comfort and other performances in the vertical direction of the vehicle there are certain vehicle models that are used in industry, ranging from a simple quarter car model(figure 2.5) to a full car model(figure 2.7). These models are modelled using spring mass damper systems. The full car model(figure 2.7) has been included here to show the different types of models used in the industry, but for this thesis work done, a simple linear half car model is sufficient to solve the problem statement in the concept phase.

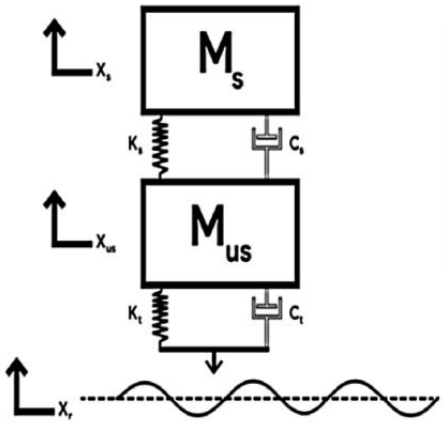

Figure 2.5: Quarter Car Model[11]

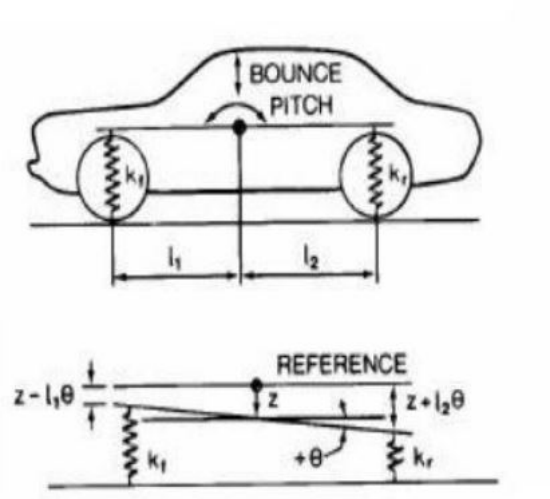

Figure 2.6: Half Car Model representing pitch and bounce motion only[11]

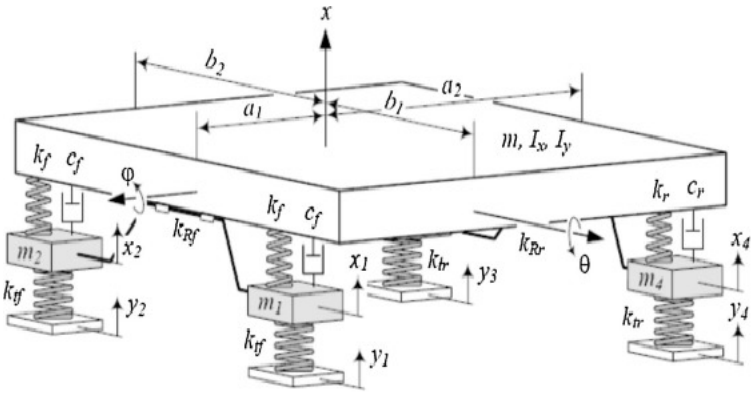

Figure 2.7: Full Car Model[15]

2.6 Human Perception to vibration

The human body is physically and biologically a system of complex nature. When looked upon as a Mechanical system, a certain number of linear and nonlinear elements can be considered and the mechanical properties differ from person to person. Even though it is not possible to consider a human as a mechanical system in real life, using this method we can see the different parts of the body that are affected at different frequency ranges[9]. When investigating the human response to vibrations and shocks, both mechanical and psychological factors should be considered. The ultimate objective is to avoid shocks from influencing the human body, therefore it is essential to understand the human response to the vibration characteristics.

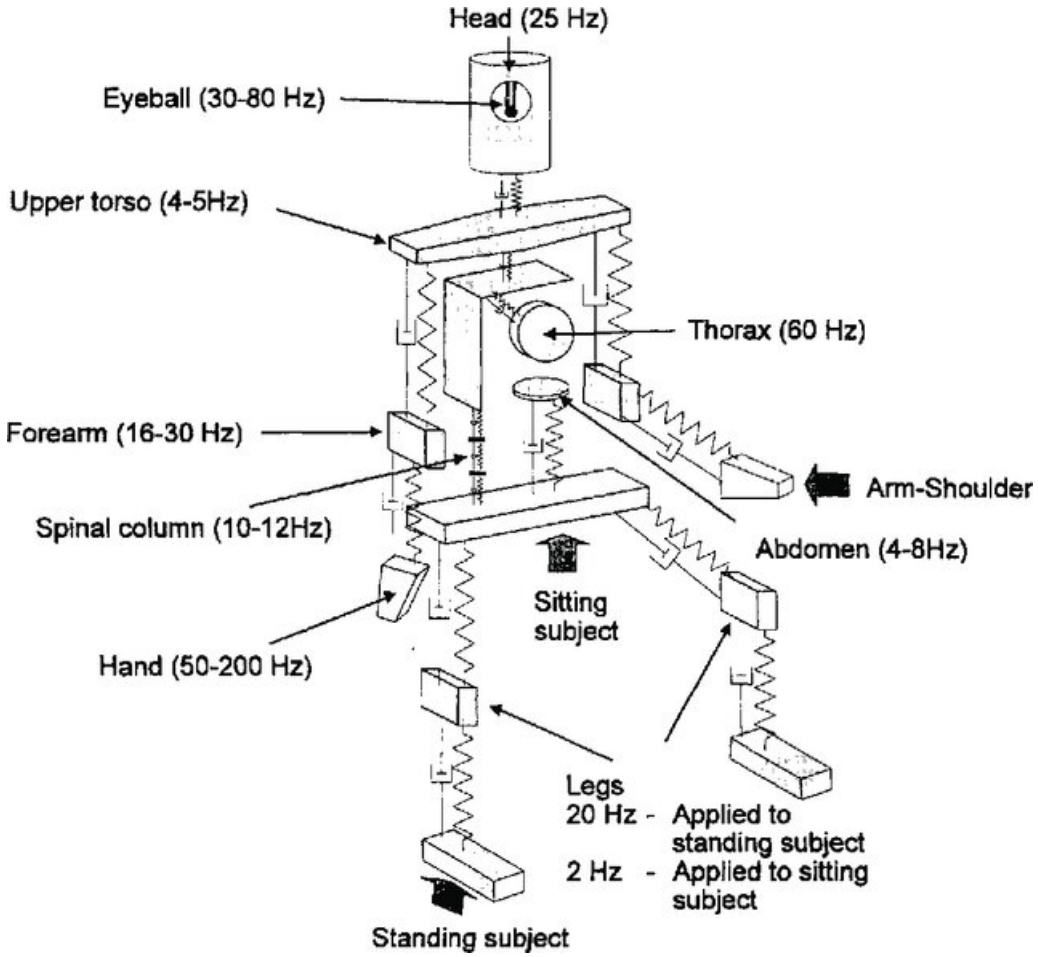

Figure 2.8: Human Body as a Mechanical System[13]

Griffin et al.[7] states that the influence of vibration on the human body is determined by the intensity of vibration, duration of vibration,human body type,seating posture and so on. In the region of choppiness(4-8Hz) the human body is found to have the lowest tolerance to whole body vibrations(SS Rao et al.)[13], from the above figure it can be seen that the abdomen region is affected at 3-8 Hz, showing an effect of choppiness. A resonance effect in the range of 20-30 Hz can be felt in the head and neck region, with eyeballs detecting a resonance effect close to 90 Hz.

Physiological and psychological effects are also observed due to the exposure of vehicle vibration. Vehicle Vibration impacts the cardiovascular health conditions such as change in heartbeat, it also induces muscle contraction and suppression of motor reflexes which ultimately leads to fatigue in the body. At lower frequencies around 1-1.5Hz i.e. in the primary ride region,vehicle vibration results in motion sickness. Continuous exposure to whole body vibrations also cause speech disturbances and lower back aches.

2.6.1 ISO standards

The International organisation for standardization(ISO) provides guidelines, requirements and specifications that have to be followed for certain products and different industries. The ISO standards also provide guidelines for evaluating the human health, human comfort levels and exposure to mechanical vibrations. The ISO 2631 standard consists of several sections, each focusing on different aspects of vibration evaluation. In this thesis we consider the guidelines for the evaluation of human exposure to whole body vibration. There are three human exposure to human vibration, namely (ISO 2631, second edition) :

- Vibrations transmitted to the whole body or substantial parts of it.
- Vibrations transmitted to the body as a whole through a supporting surface like the buttocks of the a seated person in a vehicle.
- Vibrations applied to particular parts of the body such as limbs or head.

The ISO 2631 standards also suggests two metrics to quantify the ride comfort level in a vehicle, which are the root mean square acceleration and vibration dose value. The RMS acceleration is given by the formula:

$$a_{rms} = \sqrt{\frac{1}{N_0}\sum_{n=1}^{N_0} a^2} \tag{2.1}$$

where a is the weighted acceleration and N_0 is the total number of values present.

The vibration dose value(VDV) is given by:

$$a_{vdv} = (\int_0^T a^4(t)dt)^{1/4} \tag{2.2}$$

where a is the weighted acceleration and T is the total measurement period in seconds.
To evaluate the ride comfort of the vehicle, these are the two values that are used in the industry. The weighted acceleration is calculated by using the human filter function from the table provided by ISO 2631.

Frequency f Hz	w_k factor ×1 000	w_k dB
0,02		
0,025		
0,031 5		
0,04		
0,05		
0,063		
0,08		
0,1	31,2	−30,11
0,125	48,6	−26,26
0,16	79,0	−22,05
0,2	121	−18,33
0,25	182	−14,81
0,315	263	−11,60
0,4	352	−9,07
0,5	418	−7,57
0,63	459	−6,77
0,8	477	−6,43
1	482	−6,33
1,25	484	−6,29
1,6	494	−6,12
1,6	494	−6,12
2	531	−5,49
2,5	631	−4,01
3,15	804	−1,90
4	967	−0,29
5	1 039	0,33
6,3	1 054	0,46
8	1 036	0,31
10	988	−0,10
12,5	902	−0,89
16	768	−2,28
20	636	−3,93
25	513	−5,80
31,5	405	−7,86
40	314	−10,05
50	246	−12,19
63	186	−14,61
80	132	−17,56
100	88,7	−21,04
125	54,0	−25,35
160	28,5	−30,91
200	15,2	−36,38
250	7,90	−42,04
315	3,98	−48,00
400	1,95	−54,20

Figure 2.9: Human Filter Function for vertical vibrations from ISO 2631[10]

2.7 Choppiness

Choppiness is an aspect of ride comfort and it is felt in the secondary ride frequency region of 3-8 Hz. It can be defined as continuous road induced, irregular pitch and bounce motions of the vehicle just above the primary ride frequency range. Choppiness is prevalent when driving over a uneven or rough road surface than when driving on a smooth road surface. Choppiness occurs in an area where human tolerance to whole-body vibrations is poor, causing irritation in the gut/abdomen region. Speech disturbances and headaches are also caused by a high level of choppiness.

The consequences of choppiness are mostly caused by vertical forces. When compared to a standard ICE vehicle, a BEV has an increased level of vertical vibration in the 3-8 Hz frequency (choppiness) range, which can be noticed by the driver and front passenger. The ICE, together with its engine mounts, acts as a heavy mass damper, reducing vibration input to the driver and occupants' seats at 3-8Hz, whereas the electric motor is not as heavy and has less potential to reduce choppiness, hence increasing choppiness in a BEV.

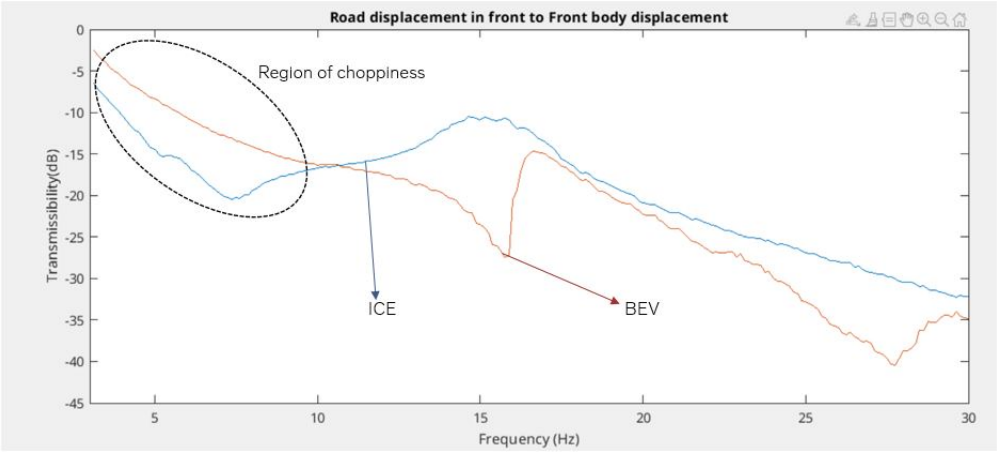

Figure 2.10: Plot explaining the difference in choppiness level between BEV and ICE

To quantify the choppiness level experienced by the driver and passengers in the vehicle, the RMS acceleration of the seat can be found between the frequency range of 3-8 Hz using the equation 2.1.

2.8 Simulation Environment

MATLAB and Simulink were used to run the various test cases on the CAE ride model.

2.8.1 MATLAB

MATLAB is a programming language from the company Mathworks, which can be used to analyse data, develop algorithms. It provides a vast number of toolboxes which allows the user to perform various operations in the field of vehicle dynamics, signal and image processing, control systems, wireless communication etc.

2.8.2 Simulink

Simulink is a toolbox in MATLAB. Simulink was built to model and simulate control systems. By using Simulink a complex system can be analysed by simulating block diagrams. The simulink library also provides a range of toolboxes which can perform operations in various fields ranging from vehicle dynamics to deep learning.

The advantages of using Simulink are as follows :

- Well proven tool in the industry and the usage of block diagrams makes it easier to understand and debug.
- Non linear models and linear can be easily modelled.
- As the simulation is done over time the state of the system can be viewed in a specific time slot. A specific start and stop time can be given for the model to run between to obtain the respective solution.

3 Methodology

3.1 CAE Ride Models

To address the problem statement, an analytical approach based on mathematical models of two vehicles was adopted. A 7-seater large SUV with an ICE and a 5-seater mid-size SUV with an electric powertrain were chosen as the two vehicles. Two vehicles were chosen to compare the choppiness levels in both the vehicles and understand the various factors affecting the choppiness in a conventional ICE vehicle and a battery electric vehicle. for both the vehicles, detailed half car models in the longitudinal direction were studied. The choice of a half car model was made in order to keep the ride model as simple as possible in order to understand the numerous aspects causing choppiness and find out solutions to reduce choppiness by improving the seat parameters.

3.1.1 ICE vehicle ride model

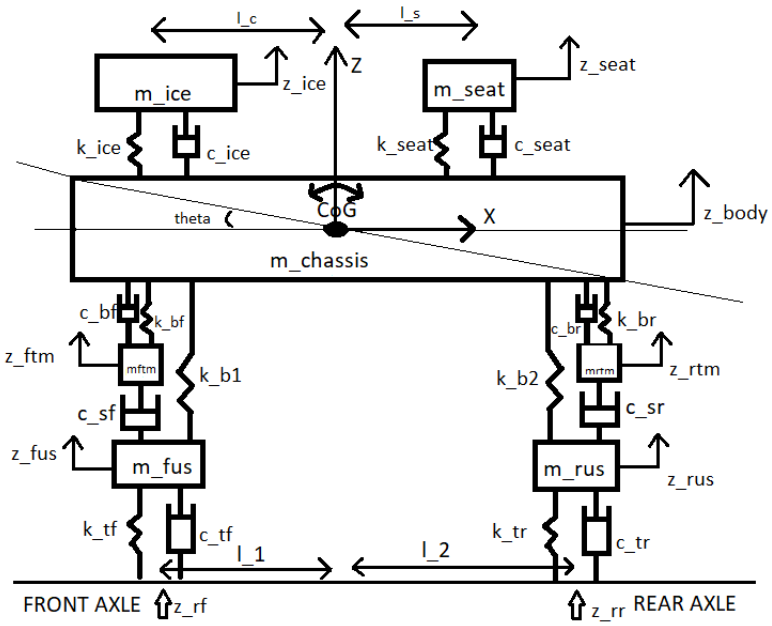

Figure 3.1: Ride model of a conventional ICE powertrain vehicle

The above figure depicts the ride model of an ICE vehicle. The half car model is made up of the 7 rigid mass blocks, which are the vehicle body, the engine, the vehicle seat, front and rear top mounts, and the front and rear unsprung masses. The entire vehicle is modelled as a spring mass damper system, with the stiffness and damping coefficients of each component considered in the vertical direction. The bushings of the engine mounts, top mounts, the tires, suspension and shock absorbers are modelled as spring damper systems. The model consists of 8 degrees

of freedom, 7 translational and 1 rotational movement. The translational movements are all in the vertical(z direction), these are the vertical bounce motion of vehicle body, engine, seat, front and rear top mounts as well as the front and rear unsprung masses, where as the rotational motion is the pitch motion of the vehicle body around the y direction.

3.1.2 Electric vehicle ride model

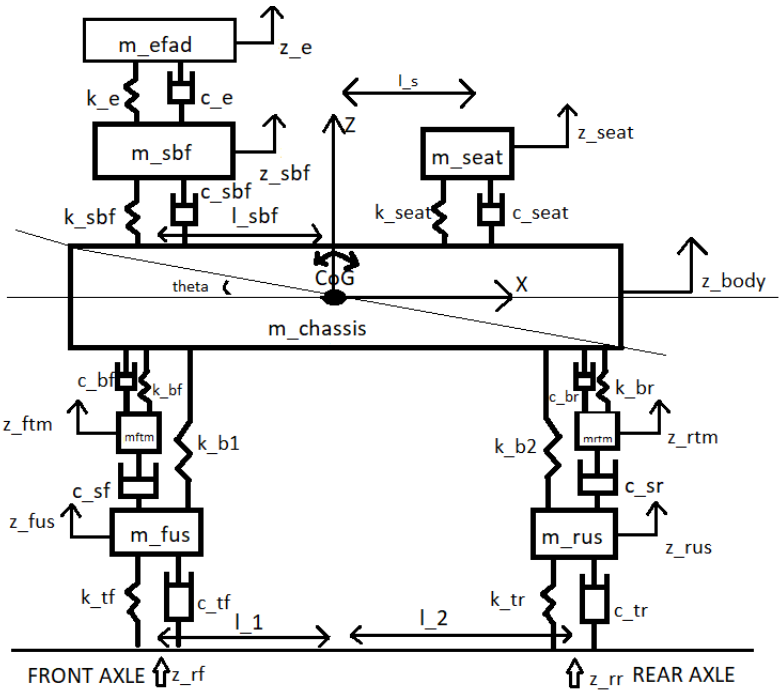

Figure 3.2: Ride model of an electric powertrain vehicle

The BEV is also modelled as a half car model. The model is made up of the 8 rigid mass blocks, which are the vehicle body, the electric motor, the subframe, the vehicle seat, front and rear top mounts, and the front and rear unsprung masses. The BEV has 9 degrees of freedoms, 8 translational and one rotational motion. The translational movements are all in the vertical(z direction), these are the vertical bounce motion of vehicle body, electric motor, sub-frame, seat, front and rear top mounts as well as the front and rear unsprung masses, where as the rotational motion is the pitch motion of the vehicle body in the y direction. The main difference between the two models is that there is a subframe present in the BEV ride model, where the electric motor is mounted.

Variables	Description
m_{seat}	Mass of seat
m_b	Mass of vehicle body
m_e	Mass of electric motor
m_{sbf}	Mass of subframe
m_{ice}	Mass of engine
m_{ftm}	Mass of front top mount
m_{rtm}	Mass of rear top mount
m_{fus}	Mass of front unsprung mass
m_{rus}	Mass of rear unsprung mass
I_{yy}	Moment of Inertia in y direction

Table 3.1: Mass and moment of inertia parameters for both the ride models

Variables	Description
l_e	Distance of electric motor and subframe from CoG
l_c	Distance of ICE from CoG
l_s	Distance of the seat from CoG
l_1	Distance of front axle from CoG
l_2	Distance of rear axle from CoG

Table 3.2: Lengths considered in both ride models

Variables	Description
k_{seat}	Seat stiffness
c_{seat}	Seat damping coefficient
k_{ice}	Engine mounts vertical bushing stiffness
c_{ice}	Engine mounts vertical bushing damping coefficient
k_e	Electric motor mounts vertical bushing stiffness
c_e	Electric motor mounts vertical bushing damping coefficient
k_{sbf}	Subframe vertical bushing stiffness
c_{sbf}	Subframe vertical bushing damping coefficient
k_{bf}	Front top mount vertical bushing stiffness
c_{bf}	Front top mount vertical bushing damping coefficient
k_{br}	Rear top mount vertical bushing stiffness
c_{br}	Rear top mount vertical bushing damping coefficient
k_{b1}	Front suspension stiffness
k_{b2}	Rear suspension stiffness
c_{sf}	Front shock absorber damping coefficient
c_{sr}	Rear shock absorber damping coefficient
k_{tf}	Front tire stiffness
c_{tf}	Front tire damping coefficient
k_{tr}	Rear tire stiffness
c_{tf}	Rear tire damping coefficient

Table 3.3: Stiffness and damping coefficients considered for both ride models

Variables	Description
θ	Pitch angle
z_{rf}	Road input in the front axle
z_{rr}	Road input in the rear axle
z_s	Vertical Displacement of seat
z_{ice}	Vertical Displacement of engine
z_e	Vertical Displacement of electric motor
z_{sbf}	Vertical Displacement of sub-frame
z_b	Vertical Displacement of body
z_{ftm}	Vertical Displacement of front top mount
z_{rtm}	Vertical Displacement of rear top mount
z_{fus}	Vertical Displacement of front unsprung mass
z_{rus}	Vertical Displacement of rear unsprung mass

Table 3.4: Translational and rotational movements considered for both ride models

3.2 Equations of motion

After creating the mathematical models of the two chosen vehicles, the next step is to derive the governing equations to understand the forces acting on each of the rigid mass blocks. Using Newtons second law of motion $F = m \cdot a$, the equations of motion were derived. Free body diagrams for all the rigid masses were drawn to find out the forces acting on them. Since the models have been modelled using spring mass damper systems all the equations of motion follow the basic equation: $m\ddot{z} + c\dot{z} + kz = 0$

3.2.1 ICE ride model

Since the ICE ride model has eight degrees of freedom, we will have eight equations of motions, seven for the vertical forces and one for the pitch motion of the vehicle body.

1. Equation of motion of engine :
$m_{ice}\ddot{z}_{ice} = -F_{ice}$

where $F_{ice} = k_{ice}(z_{ice} - (z_b + l_c\theta)) + c_{ice}(\dot{z}_{ice} - (\dot{z}_b + l_c\dot{\theta}))$

$m_{ice}\ddot{z}_{ice} = -k_{ice}(z_{ice} - (z_b + l_c\theta)) - c_{ice}(\dot{z}_{ice} - (\dot{z}_b + l_c\dot{\theta}))$

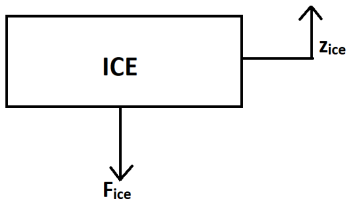

Figure 3.3: Free body diagram of engine

2. Equation of motion of seat :
$m_s\ddot{z}_s = -F_{seat}$

where $F_{seat} = k_s(z_s - (z_b - l_s\theta)) + c_s(\dot{z}_s - (\dot{z}_b - l_s\dot{\theta}))$

$m_s\ddot{z}_s = -k_s(z_s - (z_b - l_s\theta)) - c_s(\dot{z}_s - (\dot{z}_b - l_s\dot{\theta}))$

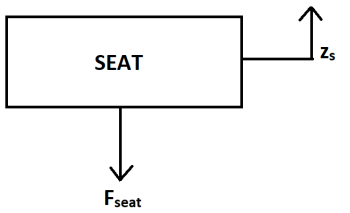

Figure 3.4: Free body diagram of seat

3. Equation of motion of front top mount:
$m_{ftm}\ddot{z}_{ftm} = F_{fronttopmount} - F_{frontshockabsorber}$

where $F_{fronttopmount} = k_{ftm}((z_b + l_f\theta) - z_{ftm}) + c_{ftm}((\dot{z}_b + l_f\dot{\theta} - \dot{z}_f tm)$,

$F_{frontshockabsorber} = c_{sf}(\dot{z}_{ftm} - \dot{z}_{ft})$

$m_{ftm}\ddot{z}_{ftm} = k_{ftm}((z_b + l_f\theta) - z_{ftm}) + c_{ftm}((\dot{z}_b + l_f\dot{\theta} - \dot{z}_{ftm}) - c_{sf}(\dot{z}_{ftm} - \dot{z}_{ft})$

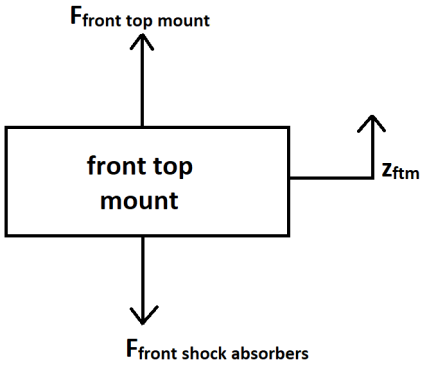

Figure 3.5: Free body diagram of Front top mount

4. Equation of motion of rear top mount :
$m_{rtm}\ddot{z}_{rtm} = F_{reartopmount} - F_{rearshockabsorber}$

where $F_{reartopmount} = k_{rtm}((z_b - l_r\theta) - z_{rtm}) + c_{rtm}((\dot{z}_b - l_r\dot{\theta} - \dot{z}_r tm)$,

$F_{rearshockabsorber} = c_{sr}(\dot{z}_{rtm} - \dot{z}_{rt})$

$m_{rtm}\ddot{z}_{rtm} = k_{rtm}((z_b - l_r\theta) - z_{rtm}) + c_{rtm}((\dot{z}_b - l_r\dot{\theta}) - \dot{z}_{rtm}) - c_{sr}(\dot{z}_{rtm} - \dot{z}_{rt})$

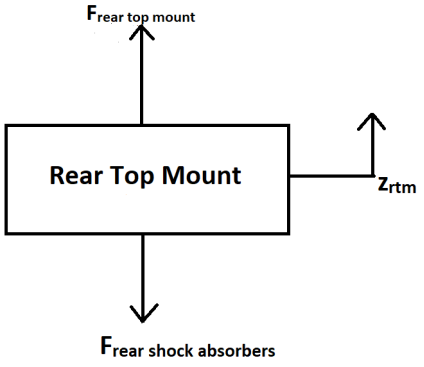

Figure 3.6: Free body diagram of Rear top mount

5. Equation of motion of front unsprung mass:
$m_{fus}\ddot{z}_{fus} = F_{frontshockabsorber} + F_{frontsuspension} - F_{fronttires}$

where $F_{frontshockabsorber} = c_{sf}(\ddot{z}_{ftm} - \ddot{z}_{ft})$, $F_{frontsuspension} = k_{b1}((z_b + l_f\theta) - z_{ft})$

$F_{frontire} = c_{ft}(\dot{z}_{ft} - \dot{z}_{rf}) + k_{ft}(z_{ft} - z_{rf})$

$m_{fus}\ddot{z}_{fus} = c_{sf}(\ddot{z}_{ftm} - \ddot{z}_{ft}) + k_{b1}((z_b + l_f\theta) - z_{ft}) - c_{ft}(\dot{z}_{ft} - \dot{z}_{rf}) - k_{ft}(z_{ft} - z_{rf})$

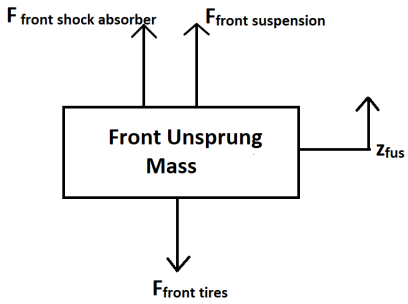

Figure 3.7: Free body diagram of Front Unsprung mass

6. Equation of motion of rear unsprung mass:
$m_{rus}\ddot{z}_{rus} = F_{rearshockabsorber} + F_{rearsuspension} - F_{reartires}$

where $F_{rearshockabsorber} = c_{sr}(\ddot{z}_{rtm} - \ddot{z}_{rt})$, $F_{rearsuspension} = k_{b2}((z_b - l_r\theta) - z_{rt})$

$F_{reartire} = c_{rt}(\dot{z}_{rt} - \dot{z}_{rr}) + k_{rt}(z_{rt} - z_{rr})$

$m_{rus}\ddot{z}_{rus} = c_{sr}(\ddot{z}_{rtm} - \ddot{z}_{rt}) + k_{b2}((z_b - l_r\theta) - z_{rt}) - c_{rt}(\dot{z}_{rt} - \dot{z}_{rr}) - k_{rt}(z_{rt} - z_{rr})$

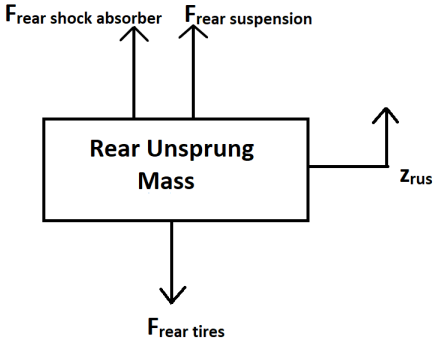

Figure 3.8: Free body diagram of Rear Unsprung mass

7. Equation of motion of vehicle body bounce:

$m_b\ddot{z}_b = F_{seat} + F_{ice} - F_{fronttopmount} - F_{reartopmount} - F_{frontsuspension} - F_{rearsupsenion}$

$m_b\ddot{z}_b = k_s(z_s-(z_b-l_s\theta))+c_s(\dot{z}_s-(\dot{z}_b-l_s\dot{\theta}))+k_{ice}(z_{ice}-(z_b+l_c\theta))+c_{ice}(\dot{z}_{ice}-(\dot{z}_b+l_c\dot{\theta}))$

- $k_{ftm}((z_b + l_f\theta) - z_{ftm}) - c_{ftm}((\dot{z}_b + l_f\dot{\theta} - \dot{z}_{ftm}) - k_{rtm}((z_b - l_r\theta) - z_{rtm}) -$

$c_{rtm}((\dot{z}_b - l_r\dot{\theta}) - \dot{z}_r tm) - k_{b1}((z_b + l_f\theta) - z_{ft}) - k_{b2}((z_b - l_r\theta) - z_{rt})$

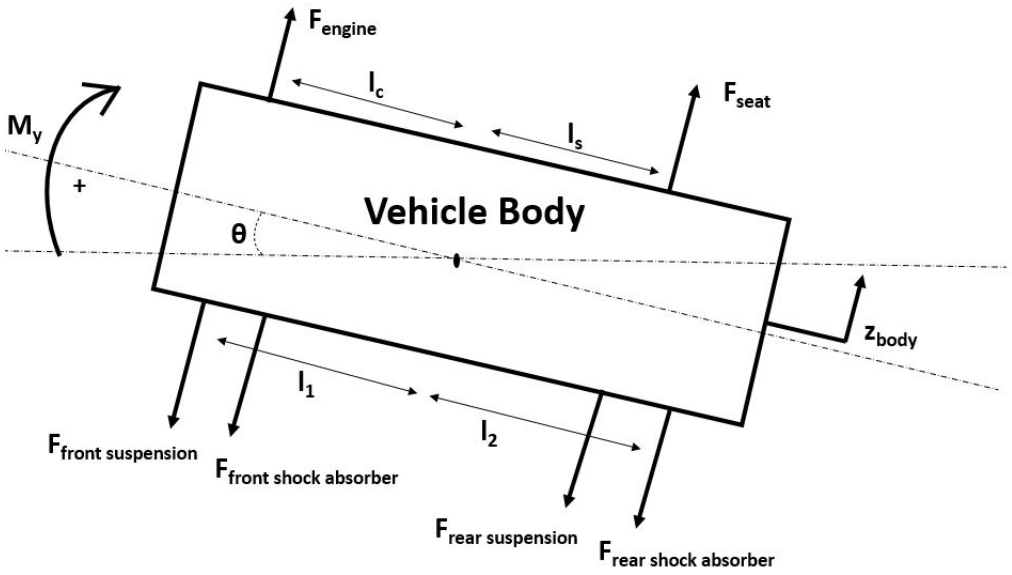

Figure 3.9: Free body diagram of Vehicle body

8. Equation of motion of vehicle pitch:

$I_y\ddot{\theta} = F_{seat} \cdot l_s + F_{ice} \cdot l_c - F_{frontsupension} \cdot l_1 + F_{rearsuspension} \cdot l_2 - F_{fronttopmount} \cdot l_1 + F_{reartopmount} \cdot l_2$

$I_y\ddot{\theta} = (k_s(z_s - (z_b - l_s\theta)) + c_s(\dot{z}_s - (\dot{z}_b - l_s\dot{\theta}))) * l_s + k_{ice}(z_{ice} - (z_b + l_c\theta))$

$+c_{ice}(\dot{z}_{ice} - (\dot{z}_b + l_c\dot{\theta})) * l_c - (k_{b1}((z_b + l_f\theta) - z_{ft})) * l_1 + (k_{b2}((z_b - l_r\theta) - z_{rt})) * l_2$

$-(k_{ftm}((z_b + l_f\theta) - z_{ftm}) - c_{ftm}((\dot{z}_b + l_f\dot{\theta} - \dot{z}_{ftm})) * l_1 + (k_{rtm}((z_b - l_r\theta) - z_{rtm})$

$-c_{rtm}((\dot{z}_b - l_r\dot{\theta}) - \dot{z}_r tm)) * l_2$

3.2.2 BEV ride Model

As the BEV ride model has nine degrees of freedom, we will have nine equations of motions, eight for the vertical forces and one for the pitch motion of the vehicle body. Because of the presence of the subframe on the vehicle body, the equations of motion of the body will have changes as the subframe and electric motor forces will act on the body in addition to the vertical bounce equations for the electric motor and subframe. The equations of motion for the two top mounts and the unsprung masses will remain the same as the ICE ride model. As a result, this section will only illustrate the free body diagrams and equations for those cases where the BEV and ICE models differ.

1. Equation of motion of electric motor :
$m_e\ddot{z}_e = -F_{electricmotor}$

where $F_{electricmotor} = k_e(z_e - z_{sbf}) + c_e(\dot{z}_e - \dot{z}_{sbf})$

$m_e\ddot{z}_e = -k_e(z_e - z_{sbf}) - c_e(\dot{z}_e - \dot{z}_{sbf})$

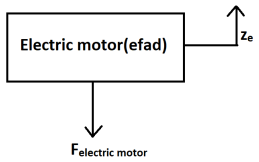

Figure 3.10: Free body diagram of Electric Motor

2. Equation of motion of subframe :
$m_{sbf}\ddot{z}_{sbf} = F_{electricmotor} - F_{subrame}$

where $F_{subframe} = k_{sbf}(z_{sbf} - (z_b + l_e\theta)) + c_{sbf}(\dot{z}_{sbf} - (\dot{z}_b + l_e\dot{\theta}))$

$m_{sbf}\ddot{z}_{sbf} = k_e(z_e - z_{sbf}) + c_e(\dot{z}_e - \dot{z}_{sbf}) - k_{sbf}(z_{sbf} - (z_b + l_e\theta)) - c_{sbf}(\dot{z}_{sbf} - (\dot{z}_b + l_e\dot{\theta}))$

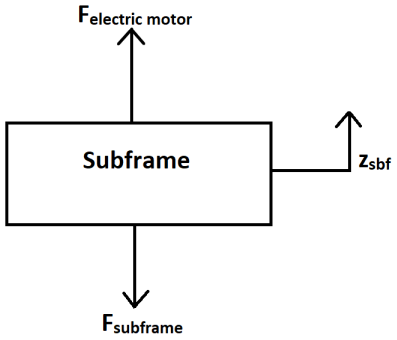

Figure 3.11: Free body diagram of Subframe

3. Equation of motion of vehicle body bounce:

$m_b\ddot{z}_b = F_{seat} + F_{subframe} - F_{fronttopmount} - F_{reartopmount} - F_{frontsuspension} - F_{rearsupsenion}$

$m_b\ddot{z}_b = k_s(z_s - (z_b - l_s\theta)) + c_s(\dot{z}_s - (\dot{z}_b - l_s\dot{\theta})) + k_{sbf}(z_{sbf} - (z_b + l_e\theta)) + c_{sbf}(\dot{z}_{sbf} - (\dot{z}_b + l_e\dot{\theta}))$

- $k_{ftm}((z_b + l_f\theta) - z_{ftm}) - c_{ftm}((\dot{z}_b + l_f\dot{\theta} - \dot{z}_{ftm}) - k_{rtm}((z_b - l_r\theta) - z_{rtm}) -$

$c_{rtm}((\dot{z}_b - l_r\dot{\theta}) - \dot{z}_r tm) - k_{b1}((z_b + l_f\theta) - z_{ft}) - k_{b2}((z_b - l_r\theta) - z_{rt})$

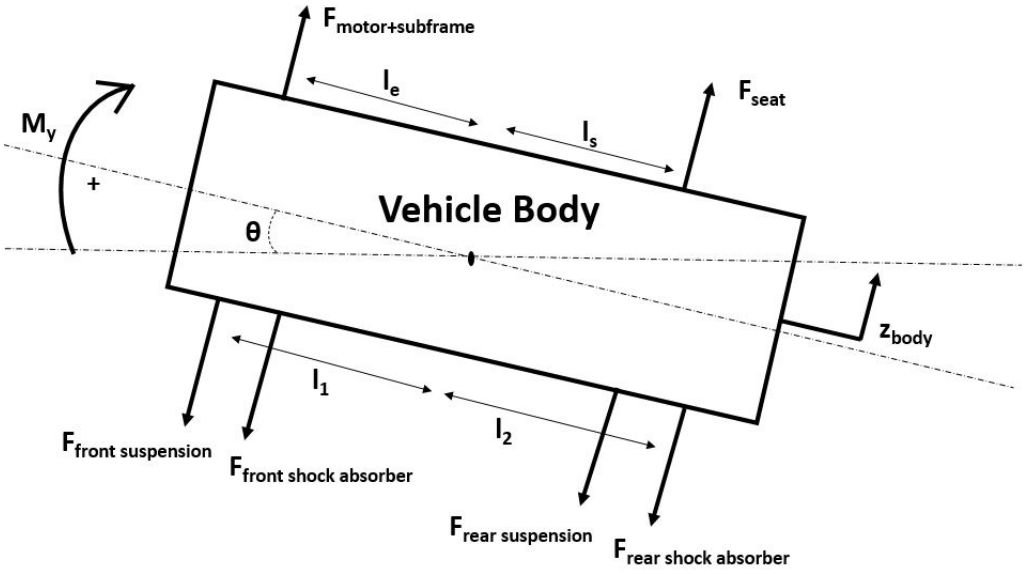

Figure 3.12: Free body diagram of BEV Vehicle body

4. Equation of motion of vehicle pitch:

$I_y\ddot{\theta} = F_{seat} * l_s + F_{subframe} * l_e - F_{frontsupension} * l_1 + F_{rearsuspension} * l_2 - F_{fronttopmount} * l_1 + F_{reartopmount} * l_2$

$I_y\ddot{\theta} = (k_s(z_s - (z_b - l_s\theta)) + c_s(\dot{z}_s - (\dot{z}_b - l_s\dot{\theta}))) * l_s + k_{sbf}(z_{sbf} - (z_b + l_e\theta))$

$+c_{sbf}(\dot{z}_{sbf} - (\dot{z}_b + l_e\dot{\theta})) * l_e - (k_{b1}((z_b + l_f\theta) - z_{ft})) * l_1 + (k_{b2}((z_b - l_r\theta) - z_{rt})) * l_2$

$-(k_{ftm}((z_b + l_f\theta) - z_{ftm}) - c_{ftm}((\dot{z}_b + l_f\dot{\theta} - \dot{z}_{ftm})) * l_1 + (k_{rtm}((z_b - l_r\theta) - z_{rtm})$

$-c_{rtm}((\dot{z}_b - l_r\dot{\theta}) - \dot{z}_r tm)) * l_2$

3.3 Load Cases

Road inputs are critical for assessing the model's resemblance to the real vehicle, as well as for evaluating and predicting the vehicle's behavior and performance. As stated in section 2.4.1, the road models considered in this section are in the vertical direction, i.e. the vertical displacement as a function of path. As road inputs to the models, two load cases were evaluated, which are :

- Sine Wave
- Rough Road

3.3.1 Sine Wave Input

The sine wave oscillates in a smooth and periodic manner, providing for controlled and consistent input conditions. Because sine waves are mathematically well defined and predictable, using them as input to the vehicle model makes it easy to compare the model to an actual vehicle and evaluate the model's performance and characteristics of the model with various modifications. Using a sine wave with varying frequency allows us to obtain the response of the vehicle in different frequency ranges, making it easier to analyse the vehicle model's response in the frequency domain. To understand the model's behaviour in both the primary and secondary ride regions, a frequency range of 0-30 Hz was selected as the start and end frequencies of the sine wave. Since the tire was modelled as a spring and damper system, vertical displacement and vertical velocity were taken as inputs into the model.

The sine wave was calculated using the formula :

$$Sinewave = Asin(2\pi f + \theta) \tag{3.1}$$

The frequency, f was calculated using the formula given below:

$$f = 10^{((((log(f_{Start}+Span)-log(f_{Start}))/(n-1))(x-1))+log(f_{Start}))} \tag{3.2}$$

where θ is the phase, A is the peak velocity amplitude, f_{start} is the start frequency and Span is the frequency range, n is the duration of the sine sweep.

The sine sweep was done for a duration of 75 seconds. The sweep was done for a short duration in order to keep the simulation time to a minimal and also receive accurate results. The velocity vs time input signal was found by using the equation 3.1 and then the integration was performed to obtain the displacement vs time input signal.

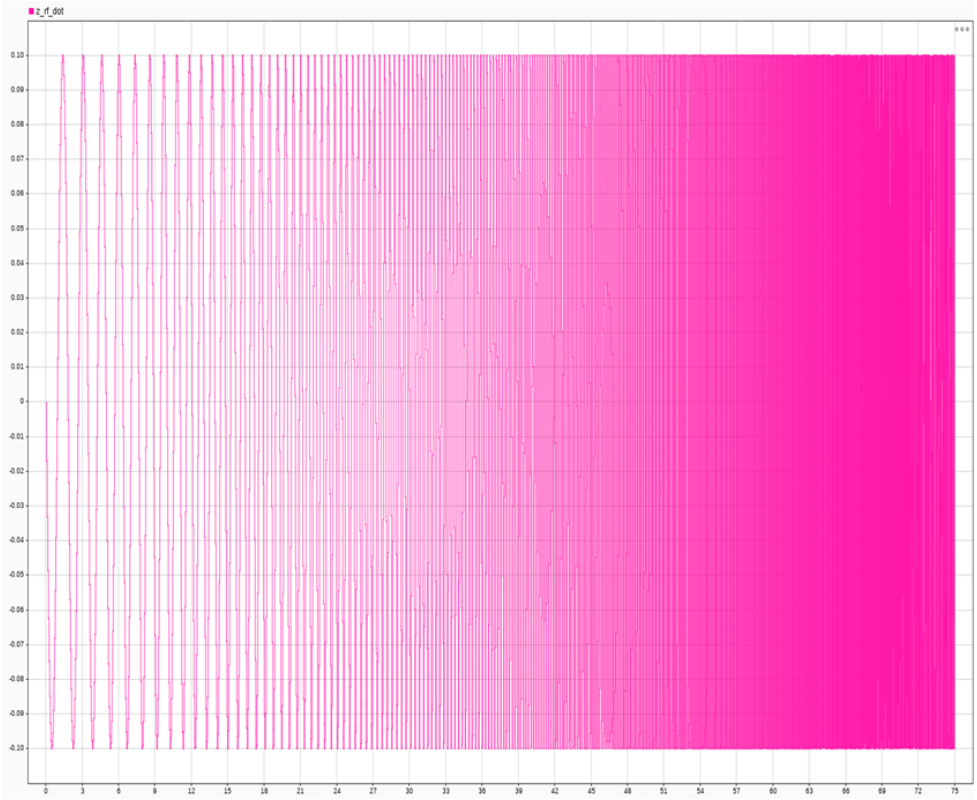

Figure 3.13: Velocity(m/s) vs time(seconds) graph for a sine wave

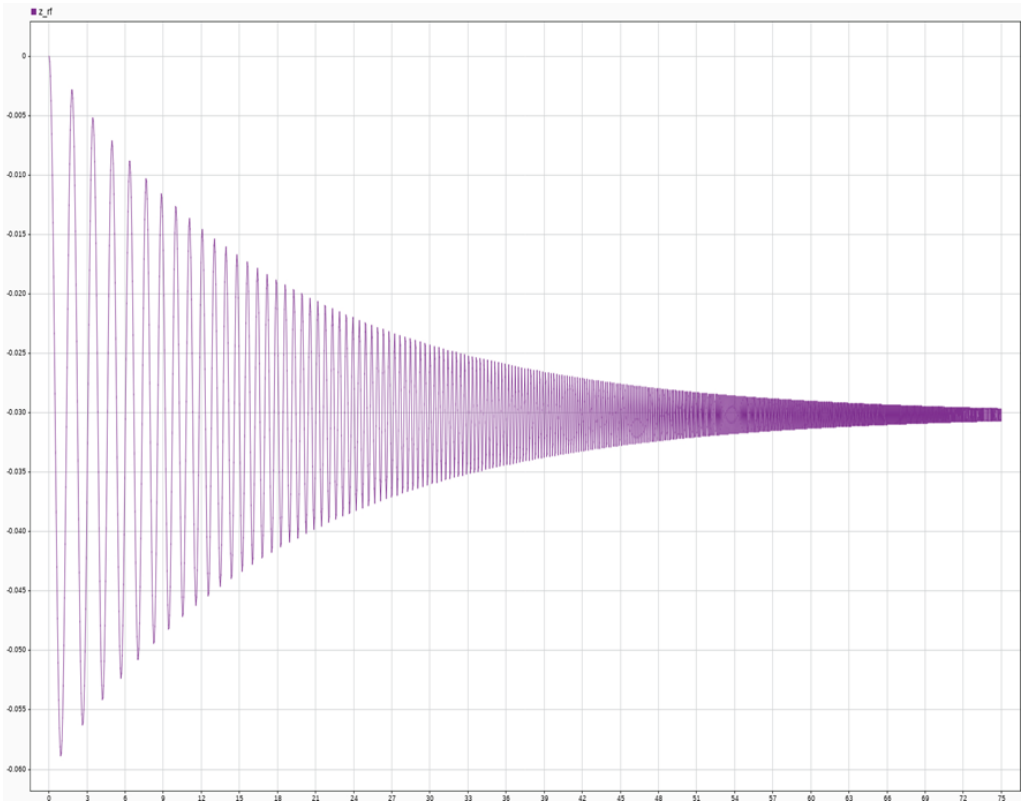

Figure 3.14: Vertical displacement(m) vs time (seconds) graph

3.3.2 Rough Road Input

To conduct a thorough ride comfort study it is important to consider an actual or real road model as well. As previously stated in section 2.7, choppiness is more prevalent when the road is rough, irregular, and uneven. Therefore, for understanding the effects of choppiness, the rough country side road used for testing has been considered. The road has been scanned when a test vehicle was driven over the test track. The signals have been calculated by Volvo Cars and a vertical displacement vs time graph for the front and rear axles have been calculated with a time lag indicating the effect of wheelbase filtering. This road input model indicates a real driving scenario thereby allowing a comprehensive study of the vehicle model and identifying areas where improvement can be made to improve the choppiness in the driver seat. The signal had to be recalculated according to the wheelbase of the two respective vehicles chosen in this thesis.

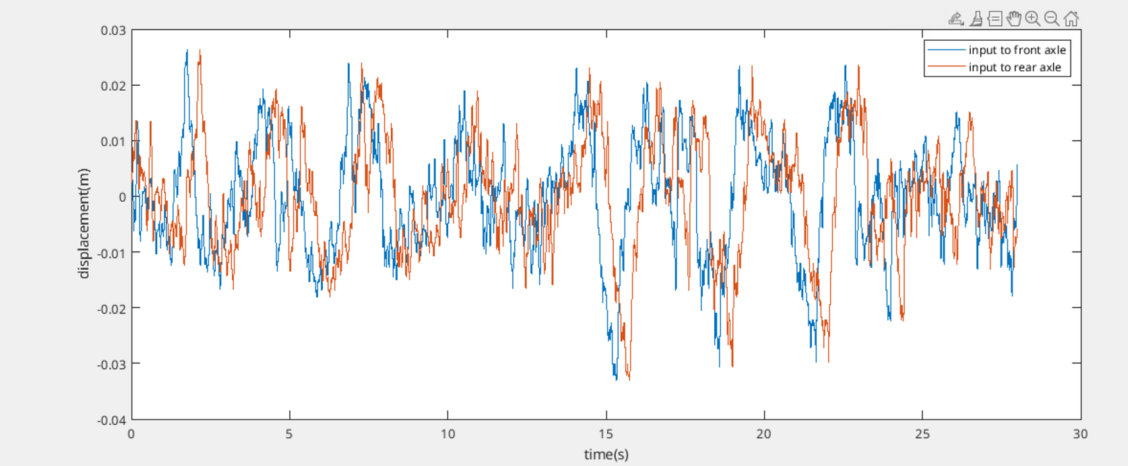

Figure 3.15: Vertical displacement(m) vs time(seconds) graph for the rough country road

3.4 Shake rig test

3.4.1 Test rig setup

It is important to compare and validate the results obtained from the ride models with those acquired from actual vehicle tests. A test vehicle with a comparable configuration to the chosen ICE vehicle, a 7-seater big SUV with an ICE, was chosen. The vehicle was placed on the test rig with accelerators placed on different locations of the vehicle. The accelerometer were placed on the following locations : On top of the engine, on the skid pad, on the wheels of the vehicle, on the seat rail, on the vehicle body i.e on the front and rear axle, on the driver. A special bracket was made to mount the accelerometer on the driver, the bracket was placed on the belt buckle of the driver.

3.4.2 Test procedure

Two tests were conducted on the test rig. A sine wave was given as the input signal. The duration of the procedure was fifteen minutes. The test was done with a driver and one passenger in the front passenger seat always. Three trials were conducted for each test where the driver and passenger were interchanged. The first test was performed with the sine wave input solely in the front axle and no input in the rear axle. During this test, the accelerometer was mounted on the car at the front axle, directly above the fender, and solely on the front two wheels, as well as the other locations listed above. During this test, the accelerometer was mounted on the car at the rear axle, above the fender, and the rear two wheels, as well as the other points described above.

Figure 3.16: Driver with accelerometer on the belt buckle

Figure 3.17: Test vehicle on the test rig

Figure 3.18: Accelerometers mounted on the skid pad, front body and front wheel

3.5 Simulink Model

The Simulink model representing the the CAE ride models(mathematical models) of the two chosen vehicles were built using blocks such as integrator, gain etc. The equations of motions were modelled in Simulink. The equations were modelled using newton's law of motion. The integrator block was used to integrate the acceleration of a degree of freedom to find the velocity and subsequently the displacement as well. An example model showing the equation of motion of the seat modelled in simulink is shown in figure 3.19.

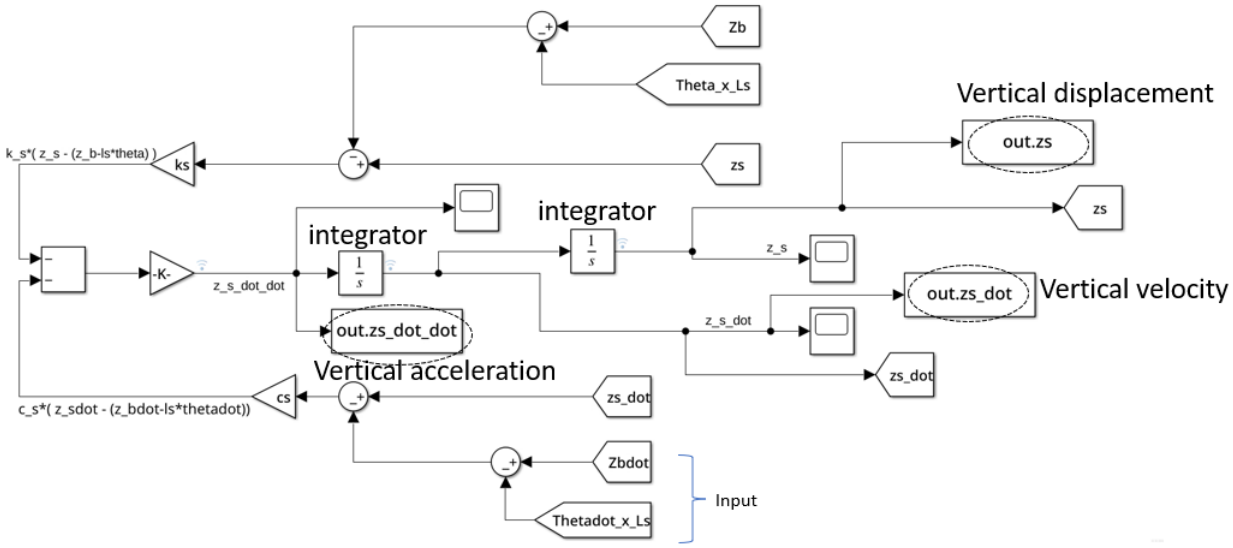

Figure 3.19: example block in simulink showing equation of motion of seat

4 Model Validation

The Simulink model of the ride models was validated after it had been developed by providing the sine wave input used in the shake rig with identical amplitude and frequency ranges as road inputs. The model was validated in the time and frequency domain. By performing these validations it was also possible to understand the effects of different parameters on the vehicle's choppiness levels.

4.1 Time Domain Response

The time domain response was necessary to understand the vehicle response to the inputs and if the vehicle's movement in the vertical direction followed the input. This was done to understand if the outputs from the vehicle body was similar to what the driver had felt while sitting in the vehicle during the shake rig tests.

4.1.1 ICE ride model

The two graphs indicate the ICE vehicle model's body response and front unsprung mass response respectively when the sine wave input is applied exclusively to the front tires. The figure 4.1 depicts the vertical displacement of the vehicle body with respect to time, it is clear from this that the model's response was very similar to what the driver experienced, as the body has a higher displacement than the input in the low frequency regions, and as time progressed during the test and at higher frequencies, the body movement in the vertical direction was minimal. The figure 4.2 depicts the vertical displacement of the front unsprung mass as a function of time. From the figure it can be seen that the unsprung mass follows the input into the vehicle for the majority of the time except at higher frequencies, this region where the vertical displacement of the unpsrung mass is higher than the sine input which is caused by wheel hop.

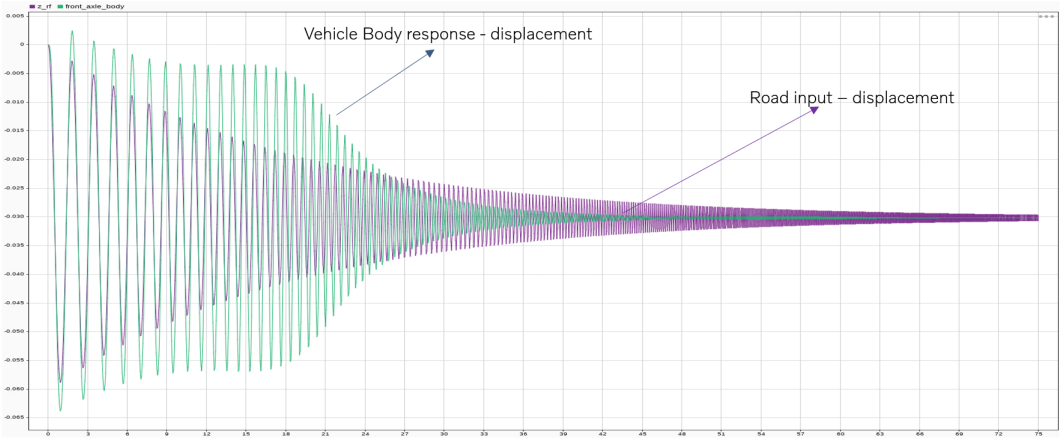

Figure 4.1: Vertical displacement(m) vs time(seconds) for ICE vehicle model's body response compared with the displacement input in front wheel

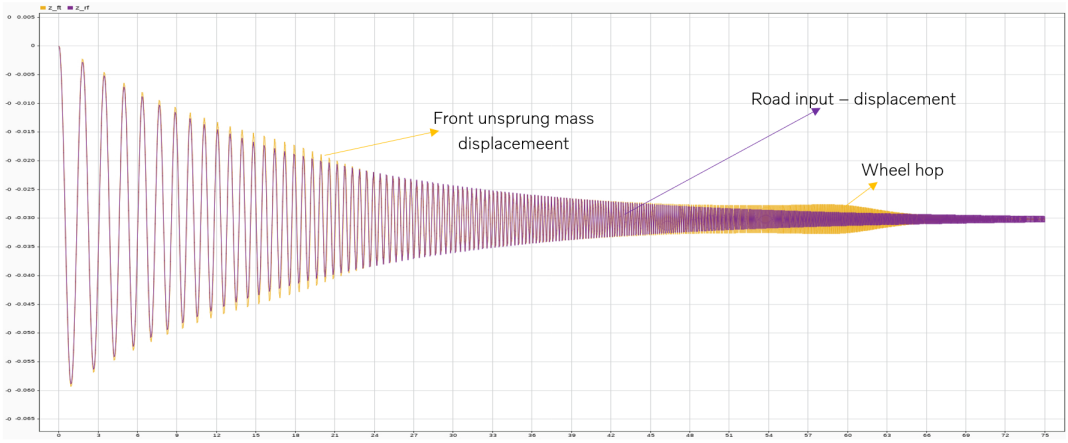

Figure 4.2: Vertical displacement(m) vs time(seconds) for ICE vehicle model's unsprung mass response compared with the displacement input in front wheel

4.1.2 BEV ride model

The BEV ride model (figure 3.2) was subjected to the same sine input as the ICE ride model applied at the front wheel. The similar response characteristics from the vehicle model was observed as that of the ICE ride model. The figure 4.3 depicts the vertical displacement of the BEV's body with respect to time, it is clear from this that the model's response was very similar to what was seen in the ICE model, the major difference only being in the amplitude levels of the body. The figure 4.4 depicts the vertical displacement of the BEV's front unsprung mass as a function of time which is again very similar to the ICE ride model's response in the vertical direction.

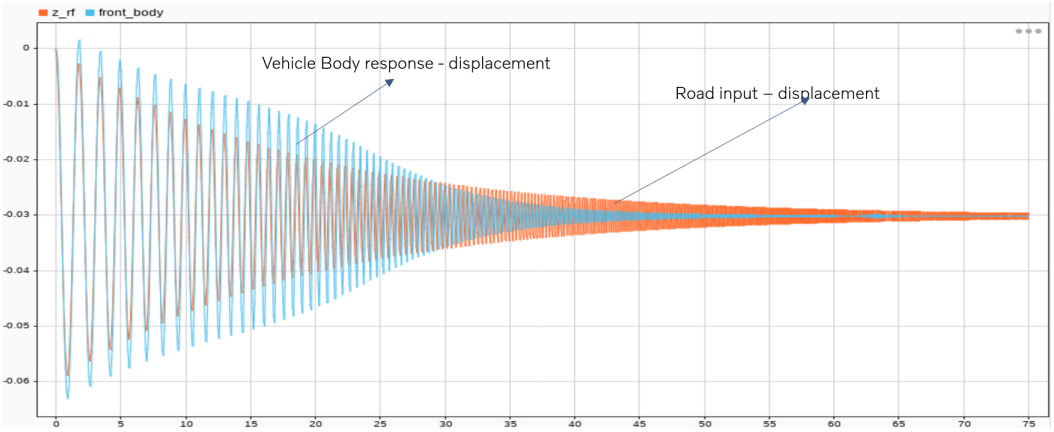

Figure 4.3: Vertical displacement(m) vs time(seconds) for BEV vehicle model's body response compared with the displacement input in front wheel

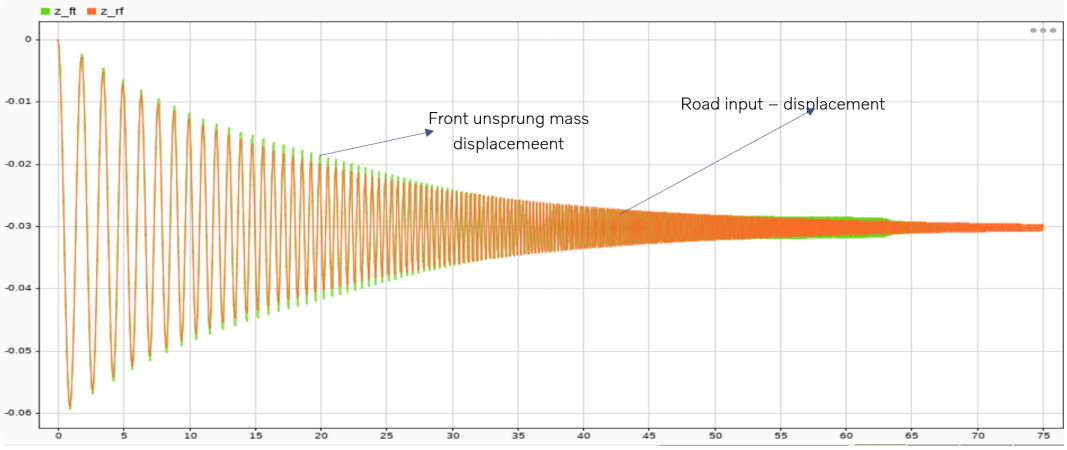

Figure 4.4: Vertical displacement(m) vs time(seconds) for BEV vehicle model's unsprung mass response compared with the displacement input in front wheel

4.2 Frequency Domain Response

The time domain response of the model does not reflect the frequencies at which wheel hop, powertrain bounce, and other factors influence the seat vertical frequency and choppiness levels in the vehicle. These effects can conveniently studied by the help of transmissibility plots, commonly known as bode plots. These plots provide an intuitive way of understanding the response of vehicle model in different frequencies. By plotting the magnitude of the transfer functions of the models in a logarithmic scale, it makes it easier to understand the resonance peaks,gain margin, behaviour of the vehicle model in dominant frequencies etc. The transmissibility plots were plotted when the input to the models were a sine wave. The frequency response of the vehicle was studied in both primary and secondary ride regions. The transmissibility plots were plotted when the input was first given to front wheels and then given to rear wheels respectively.

4.2.1 Transmissibility plots of ICE ride model

The graphs generated from the ICE ride model were compared to the plots obtained from the tests performed on the test rig with test vehicle. Four transfer functions were taken into account to study the vehicle model's response in the primary and secondary ride regions. The input for all these transfer functions was the road displacement input (sine wave) in front or rear axle. The outputs of the transfer function were the front or rear wheel vertical displacement, body vertical displacement, seat rail vertical displacement and engine vertical displacement.

The primary ride results as indicated in figure 4.5 show that the resonance peaks of the four transfer function are at the same frequency as that of the test vehicle's transfer functions. The blue curve represents the results of the Simulink model, while the orange curve represents the results of tests performed on the test vehicle on the shake rig. These results also show that there is a good correlation between

the ride model and the outcomes of the test vehicle's body transfer functions in the major ride region shortly before choppiness. It is critical to have a strong correlation between the ride model and the vehicle's body responses, because choppiness and other ride comfort issues are caused by vibration transmitted into the seat from the vehicle body.

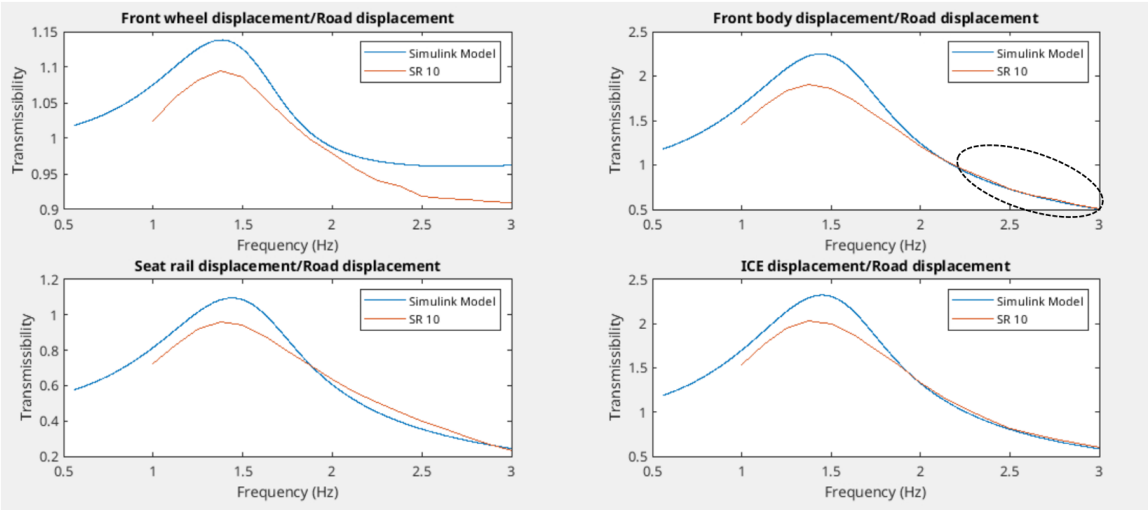

Figure 4.5: Primary ride transmissibility plots for ICE model compared with shake rig results when input is given in front axle

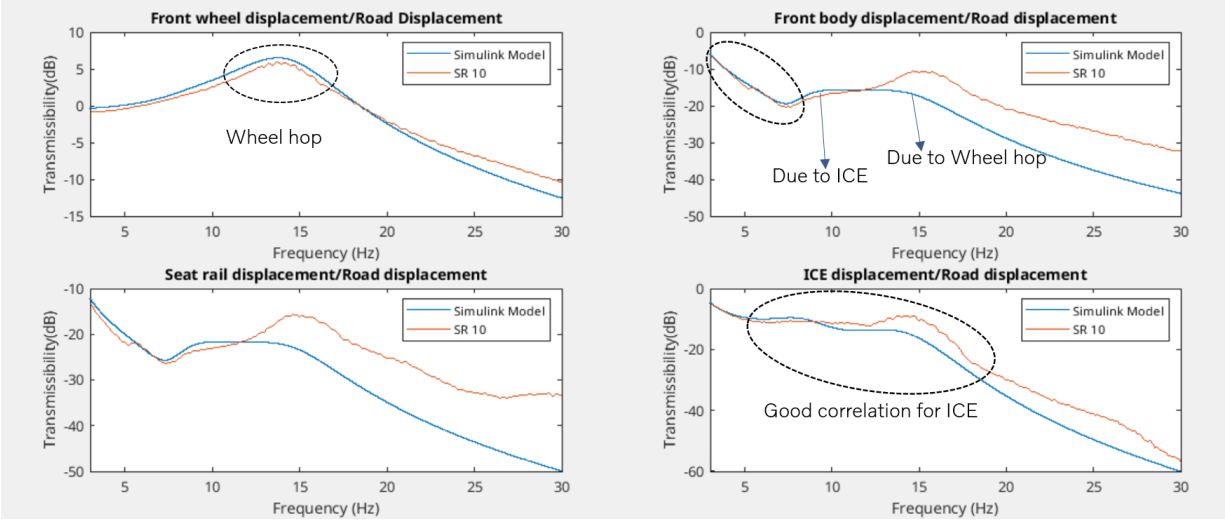

Figure 4.6: Secondary ride transmissibility plots for ICE model compared with shake rig results when input is given in front axle

The figure 4.6 shows the secondary ride plots for the ride model and test vehicle frequency responses. It can be seen from the first plot indicating the front unsprung mass response in the figure that resonance peak which is due to the wheel hop is at the same frequency for both the ride model and the test vehicle. The second plot indicates the vehicle body's response for both the ride model and test vehicle.

It can be seen that there is a good correlation between the two in the region of choppiness i.e from 3-8 Hz. It is very crucial to have a good correlation between the two, as indicated before in section 1.1 the vibrations are transmitted from the body to the seat. The ride model's body response has two resonance peaks, one is due to effect of the engine bounce and the second one is due to the effect of the wheel hop respectively. The third plot indicates the seat rail's response and it is observed that even the seat rail has a good correlation in the region of choppiness. The fourth plot represents the engine's vertical displacement(engine bounce) and it is observed that there is a good correlation between the ride model's response and test vehicle's too.

Even though the main focus of the thesis is to understand the influence of different parameters on the vehicle's choppiness levels and reduce the perceived choppiness, it is also important to understand the effects in the shake region (8-20 Hz). It was observed from the transmissibility plot of the vehicle body that the correlation between the ride model and the test vehicle was poor, and this was due to the fact the shock absorbers considered in the ride model were linear, which is not the case in real life. Therefore a huge difference between the two results was due to the fact that non linear shock absorbers with friction was not considered.

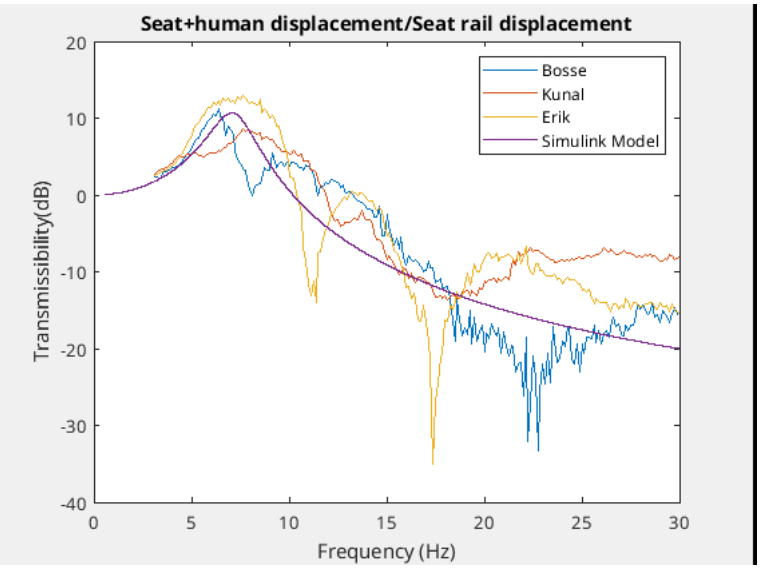

Figure 4.7: Transmissibility plots for different drivers compared with the model's response when input is given in front axle

Figure 4.7 shows transmissibility plots for the transfer function where the seat along with the driver's vertical displacement is the output where as the input is the vertical displacement of the seat rail. The purple curve represents the response from the simulink model, whilst the other curves represent the response when three separate drivers sat in the seat. The frequency response of the driver while sat in the vehicle seat was measured using an accelerometer mounted on a bracket attached to the driver's belt buckle, as illustrated in figure 3.16. According to the findings of this study, comfort levels differ from person to person because comfort is affected by a person's BMI as well as sitting position. The resonance peak of the seat from the ride model is around 6 Hz, which is within the choppiness region.

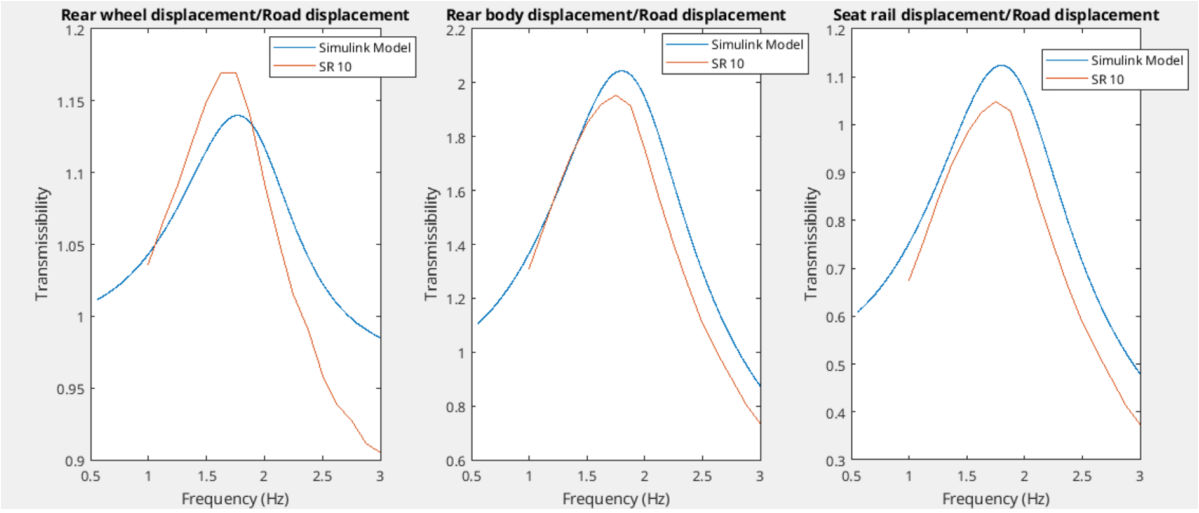

Figure 4.8: Primary ride transmissibility plots for ICE model compared with shake rig results when input is given in rear axle

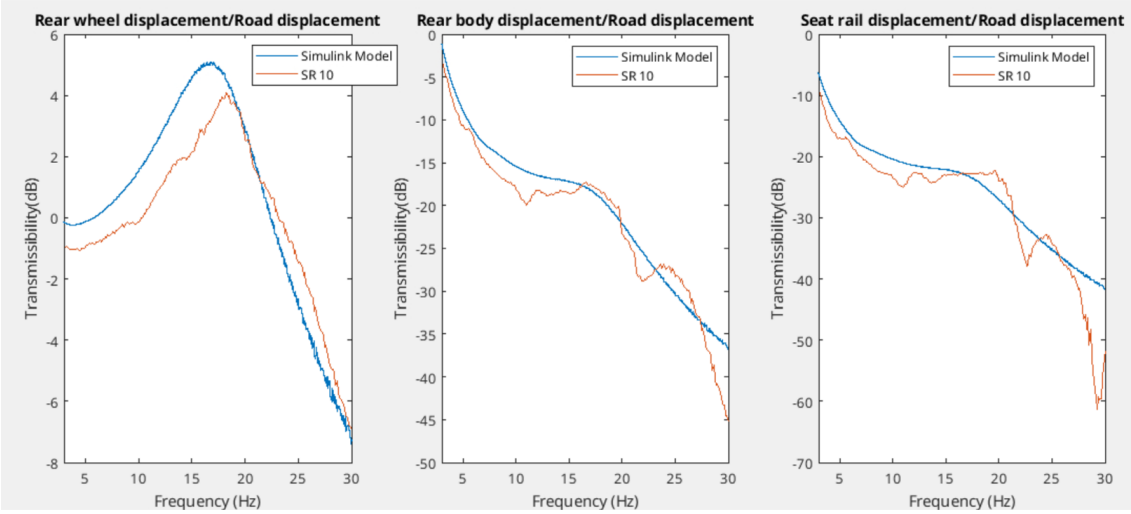

Figure 4.9: Secondary ride transmissibility plots for ICE model compared with shake rig results when input is given in rear axle

When the road input was given exclusively in the rear axle, the transmissibility plots for primary and secondary ride regions s are shown in figures 4.8 and 4.9, respectively. The blue curve shows the response of the ride model, while the orange curve indicates the response of the test vehicle. The transfer function illustrating the vertical displacement of the engine is not studied because the decibel levels are low while assessing the engine's response to the road input provided in the rear. Figure 4.8 shows that the ride model's resonance peaks in the primary ride region are at the same frequency as the test vehicle's response. The correlation between the plots of the transfer functions in the secondary ride is good, and the resonance peaks of ride models are at or near the frequency of the test vehicle.

4.2.2 Effects of Non Linearity and Friction

It was observed from figure 4.6 that linear shock absorbers did not give a good correlation between the ride model's body response and the test vehicle's body response in the higher frequency ranges. This was predominantly due to the fact the model does not have linear shock absorbers with friction models.

In order to study the effect of friction in shock absorbers, non linear shock absorbers were considered by making the dampers dependent on the vertical velocity between the top mounts and unsprung masses. Along with this non linearity a basic friction model was considered as well. A friction force of 40 N was assumed to be acting in the direction opposite of the shock absorbers's vertical movement i.e if the shock absorbers moved up a friction force of 40 N would act in the downward direction and vice versa. Figure 4.10 shows the effects of this, where the correlation between the vehicle model's body response and the test vehicle's response is better than when linear shock absorbers were utilized. The purple curve represent the response of the test vehicle, the yellow curve represents the response of the ride model with linear shock absorbers and the blue curve represents the response of the ride model with non linear shock absorbers.

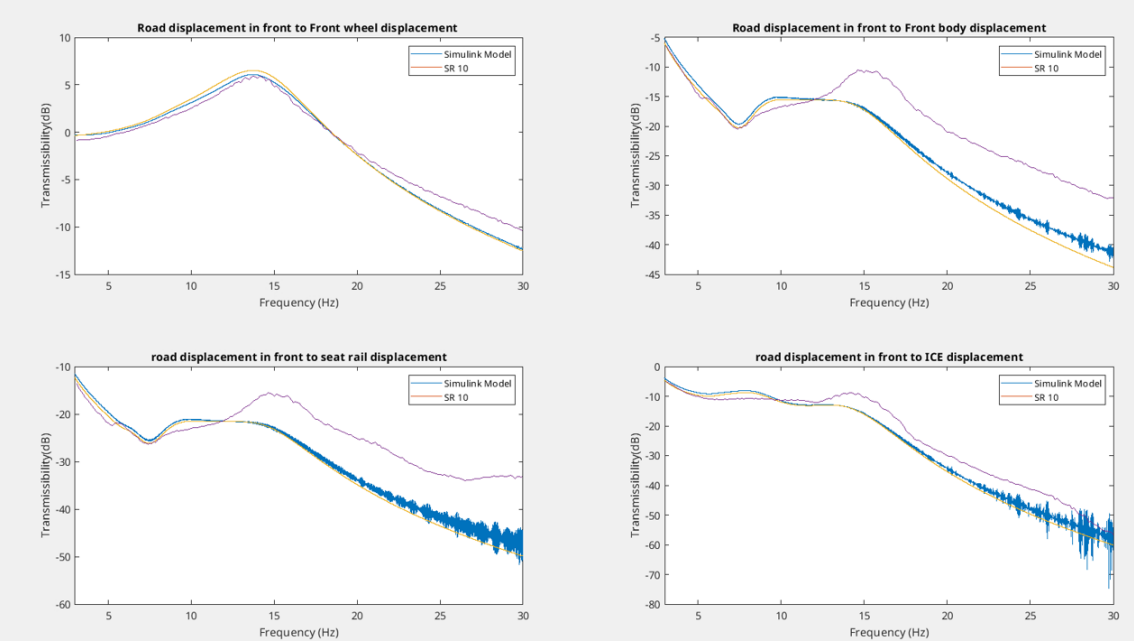

Figure 4.10: Secondary ride transmissibility plots for ICE model compared with shake rig results when input is given in front axle when friction is included in dampers

In a real-world scenario, the shock absorbers will lock in high frequency zones. To study this impact further, shock absorbers with extremely stiff values were included in the linear ride model to totally lock them. The consequence of this is seen in figure 4.11, where it can be observed that the correlation between the ride model's body reaction and the test vehicle's body response is considerably better at high frequency regions, as indicated by the black circles. Because the primary goal of the thesis was

to investigate the influence of choppiness, this model with stiff dampers was not used because the body correlation at 3-8 Hz was very poor and the resonance peaks did not match. This is indicated by the red circle over the choppiness region in the second plot which shows the transfer function of vehicle body's vertical displacement with road input. The correlation between the ride model's unsprung mass and vehicle's wheel displacement is also incorrect.

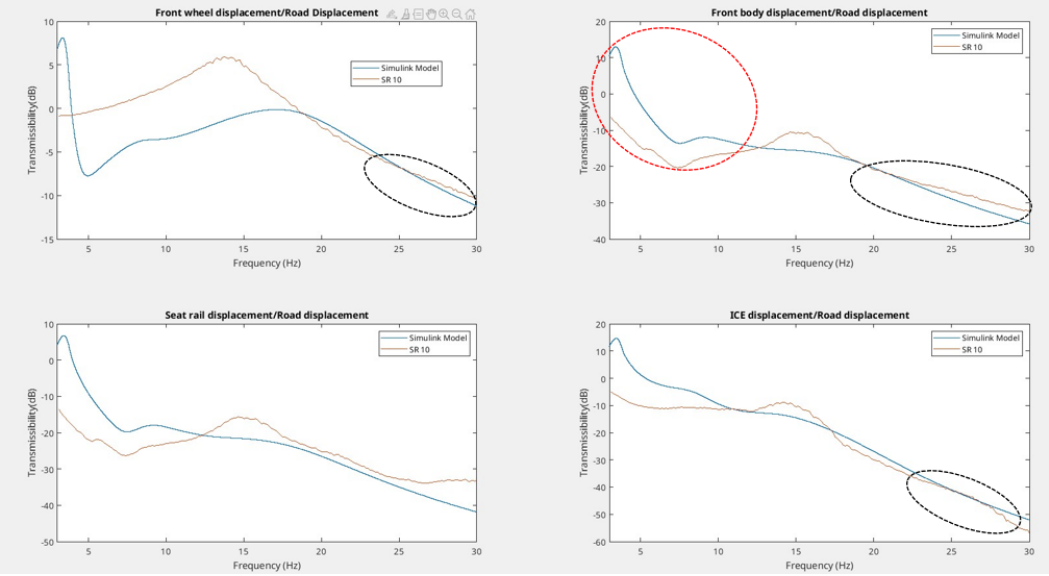

Figure 4.11: Secondary ride transmissibility plots for ICE model compared with shake rig results when input is given in front axle when dampers are locked

4.2.3 Transmissibility plots of BEV ride model

The bode plots of the BEV ride model's response were compared to the plots from tests performed on the test rig with the BEV test vehicle. Because the test vehicle was not available to conduct the testing, these results were compared to earlier work done by Volvo Cars. Four transfer functions were found from the CAE ride model once more, with the outputs being the unsprung mass vertical displacement, body vertical displacement, seat rail vertical displacement, and electric motor vertical displacement. The road displacement (sine wave) was used as the input. Because data from the other two transfer functions were not available from the shake rig measurements, only two transfer functions with outputs of unsprung mass (wheel) vertical displacement and body displacement were compared with test results in this study

The primary ride results as indicated in figure 4.12 show that the resonance peaks of the two transfer function are at the same frequency as that of the test vehicle's transfer functions. The blue curve represents the results of the Simulink model, while the orange curve represents the results of tests performed on the test vehicle on the shake rig. These results also show that there is a good correlation between the ride model and the response of the test vehicle's body transfer functions in the primary ride region shortly before choppiness which is very similar to what was

observed in the ICE ride model. In the figure the transmissibility plots of the transfer function whose output is the vertical displacement of the seatrail and electric motor is considered here to understand the frequency response of these two. It is observed that the seat rail and electric motor also have resonance peaks that are close to the body response in the primary ride which shows that the vertical movement of these two components are in sync with body's vertical displacement in the low frequency regions.

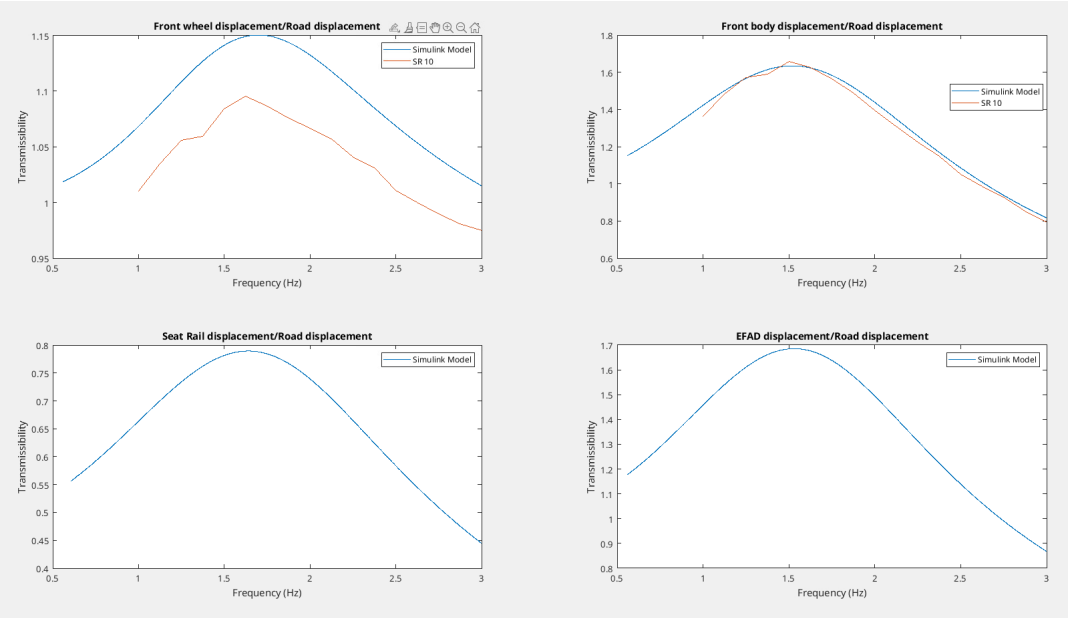

Figure 4.12: Primary ride transmissibility plots for BEV model compared with shake rig results when input is given in front axle

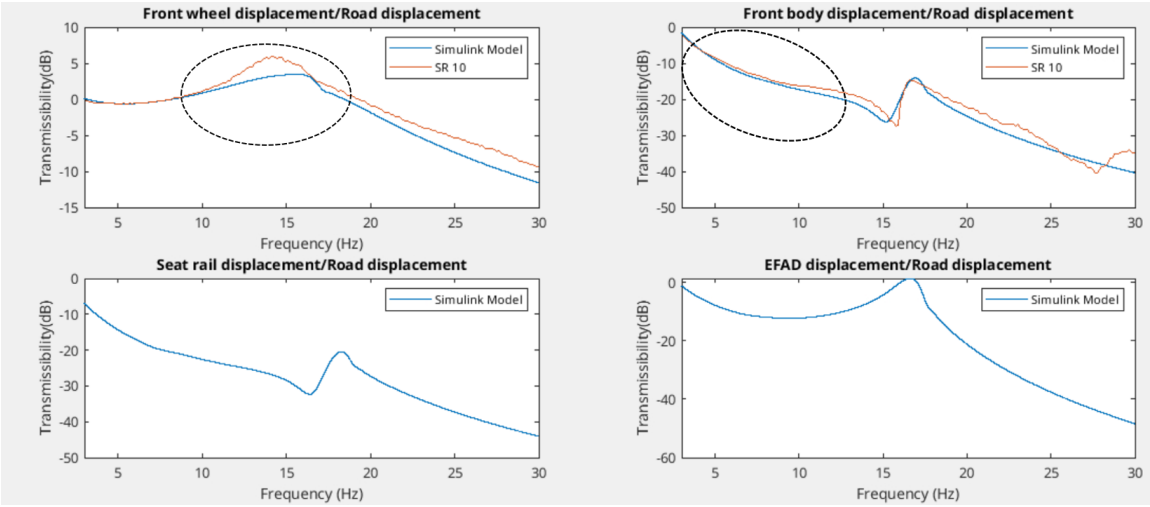

Figure 4.13: Secondary ride transmissibility plots for BEV model compared with shake rig results when input is given in front axle

The figure 4.13 depicts the transmissibility plots in the secondary ride region for the BEV ride model and test vehicle's frequency response. The first plot compares the

model's front unsprung mass response to the test vehicle's front wheel response in the frequency domain. The wheel hop frequency range is indicated by the resonance peak. The model's peak frequency is similar to the test vehicle's peak frequency. The second plot compares the vehicle body's response of the ride model and the test vehicle. There is a good correlation between the two results in the entire secondary ride region especially in the region of choppiness and also in the region of shake. There is a peak and a small dip about 15 Hz, followed by another peak at 18 Hz. The initial peak and dip in the response are caused by the electric motor's bounce, and this peak can be seen in the fourth figure, which shows the vertical response of the EFAD (electric motor in the front's response) with respect to road input. The response of the seat rail is depicted in the third plot, and it can be seen that the response of the seat rail is almost identical to that of the body, as expected.

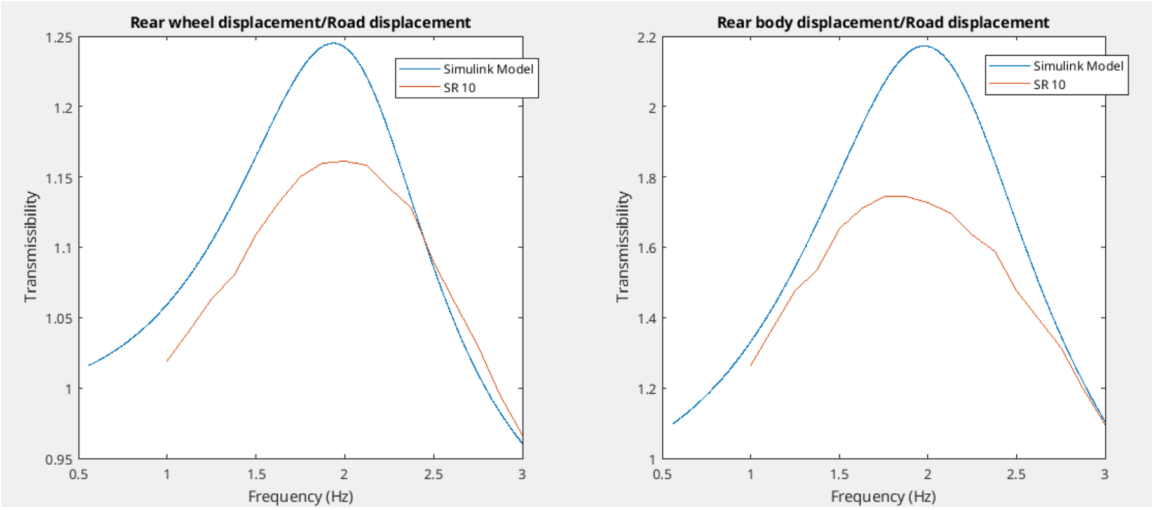

Figure 4.14: Primary ride transmissibility plots for BEV model compared with shake rig results when input is given in rear axle

Figures 4.14 and 4.15 illustrate the transmissibility plots for primary and secondary ride areas when the road input was given only in the rear axle. The blue curve represents the ride model's response, while the orange curve represents the test vehicle's response. The transfer function illustrating the vertical displacement of the electric motor and seat rail are not studied. The response of the electric motor on the front axle is not of concern because the decibel levels are low while studying the motor's response to the road input provided in the rear. Figure 4.14 shows that the ride model's resonance peaks in the primary ride region are at the same frequency as the test vehicle's response for both the rear unsprung mass and vehicle body.

Figure 4.15 depicts a comparison of the transmissibility plots of the ride model and the test vehicle in the secondary ride region. The first plot in the figure compares the ride model's rear unsprung mass response to the test vehicle's rear wheel response when the road input was applied to the rear axle. The plot shows that the peaks of the two do not have the same frequency, which is due to the fact that the test vehicle was a four wheel drive vehicle with an ERAD (electric motor in the rear), whereas the model considered for the thesis studies was a front wheel drive vehicle

with only a motor in the front. The presence of the ERAD affects the wheel hop frequency, the wheel hop frequencies of the model and test vehicle are not at the same frequency. The presence of the ERAD influences the response of the vehicle body as well. The second plot shows that the test vehicle exhibits a dip in the response about 21 Hz, this is due to the effect of ERAD's bounce. Since the ride model does not have an ERAD this dip is not seen in the ride model's response.

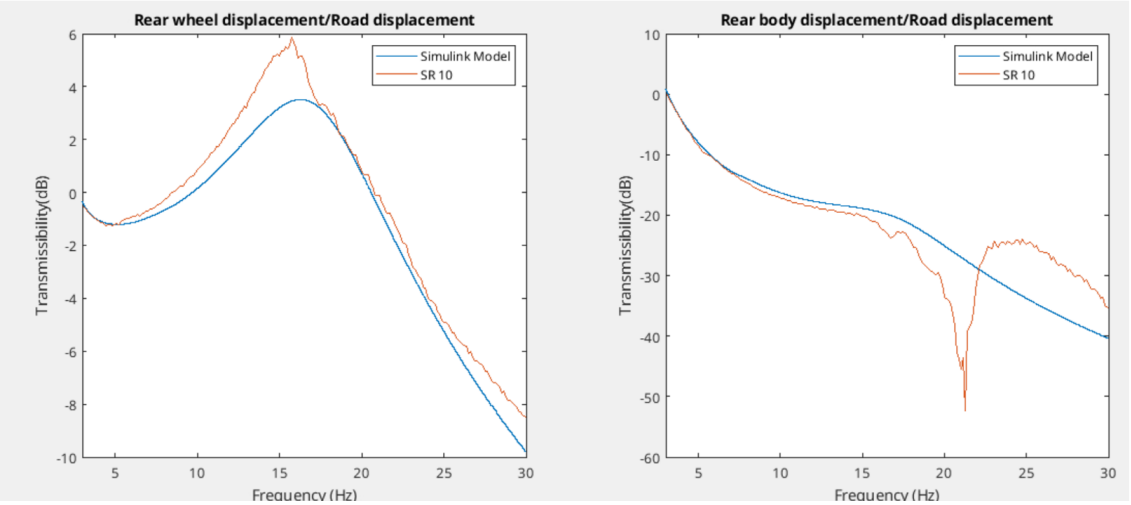

Figure 4.15: Secondary ride transmissibility plots for BEV model compared with shake rig results when input is given in rear axle

4.2.4 Effect of electric motor on choppiness

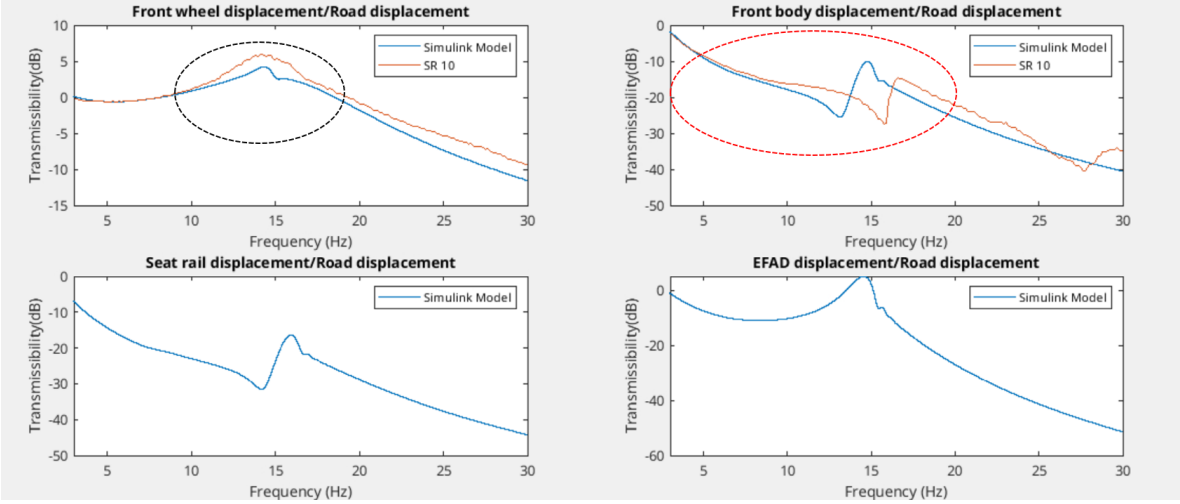

Figure 4.16: Secondary ride transmissibility plots for BEV model compared with shake rig results when input is given in front axle studying effects of EFAD bounce

Figure 4.13 illustrates a comparison of the response of the ride model and the test vehicle, demonstrating that the peak of the front unsprung mass response of the two was not at the same frequency. This was owing to the EFAD bounce effect.

The vertical stiffness and damping of the EFAD bushings were reduced to test this. Figure 4.16 depicts the vertical bounce of the EFAD on the vehicle body as well as the front unsprung mass. By reducing the stiffness and damping, it was observed that the wheel hop frequency of the ride model was similar to the test vehicle's wheel hop frequency, however the correlation between the ride model's body response to the test vehicle's body response was poor, as represented by the red circle. When compared to the test vehicle, the region where the peaks and dips appeared on the ride model's body response was at lower frequencies, affecting the correlation in the choppiness zone. The thesis focuses on improving the choppiness by adjusting the seat parameters, therefore the configuration of the ride model to achieve the results as shown in figure 4.16 was not taken into account to perform the studies to improve choppiness.

5 Results and Conclusion

5.1 Cost Function

A cost function was required to quantify the choppiness levels of a vehicle after verifying the ride models using the same inputs as used for testing the actual vehicle and understanding the impacts of various parameters on the vertical choppiness of a vehicle. The ISO 2631 standards were considered in order to do this. The RMS acceleration of the seat in the vertical direction was chosen as the cost function. The RMS acceleration was determined for the choppiness region (3-8 Hz) as well as the shake region (8-20 Hz). Although the main aim of the thesis is to improve the vertical choppiness levels in the driver seat of a BEV, it is important to examine the shake region as it is a part of the secondary ride and it is crucial to design a vehicle that is comfortable in both the regions of secondary ride.

In order to do this the weighted human filter functions (Figure 2.9) were considered. The seat acceleration response was first found in the time domain and then converted to the frequency domain.The weighted acceleration values of the seat were calculated by multiplying the acceleration readings in each frequency region by the weighting factors.

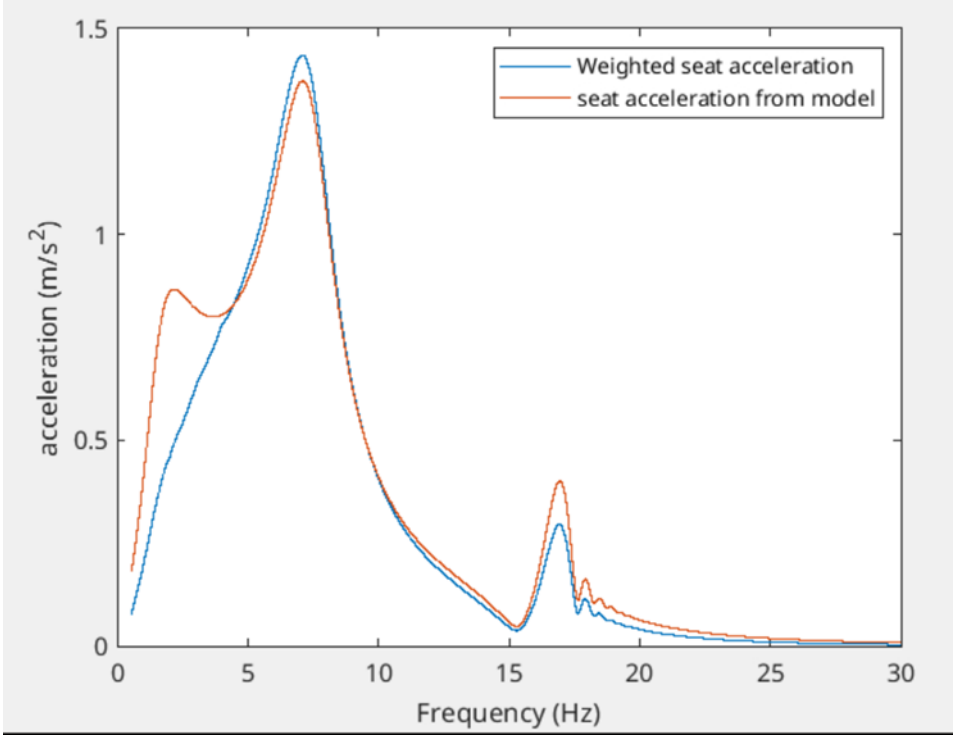

Figure 5.1: Weighted Seat acceleration

Since the cost function is the weighted RMS acceleration of the seat, the seat parameters i.e the seat stiffness and damping were the selected as the tuning parameters.

The seat stiffness and damping were altered to study the effects they have on the vertical choppiness levels on the driver seat.

5.2 RMS seat accelerations of BEV ride model

This section is divided into four subsections, the first two of which explain the changes in the cost function caused by modifying the seat parameters when the sine wave was used as an input, and the following two of which explain the findings achieved when the rough road was used as an input. As previously stated, the seat parameters for the BEV ride model were altered to determine the RMS acceleration values in the seat. The seat stiffness and damping were changed between 0.5 and 2 times the baseline value. ’

5.2.1 RMS seat acceleration in choppiness region with sine wave as road input

The seat parameters were changed across a wide range to produce a wide range of RMS acceleration values for various combinations of seat stiffness and damping. The simulation results were shown as a 3D surface plot to provide a range of RMS acceleration values from good to bad in the choppiness region. This was done to determine the path that must be taken to lower choppiness levels in a vehicle’s driver seat by modifying the seat parameters. Figure 5.2 depicts a 3D surface plot of the seat’s RMS acceleration values for various combinations of seat stiffness and damping. The green star represents the combination that results in the lowest RMS acceleration value in the choppiness region, the yellow star represents the value for low choppiness RMS acceleration value, the black star represents the baseline design, and the red star represents the combination that gives the highest RMS acceleration value in the choppiness region.

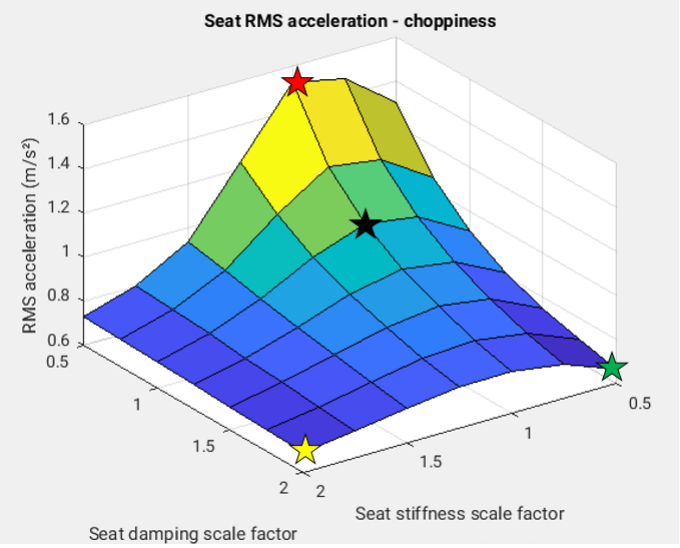

Figure 5.2: 3D surface plot showing the seat RMS acceleration in choppiness region for various combinations of seat stiffness and damping

When the seat stiffness is reduced from the baseline design and the seat damping is raised from the baseline design, the combination has the lowest choppiness levels in the seat. Stiffer seats, regardless of the damping values of the seat, help to reduce choppiness levels as well; yet, the figure shows that damping influences choppiness more than seat stiffness. The figure illustrates that the region with high RMS acceleration values for choppiness has very poor damping, despite the fact that the seats are not extremely stiff.

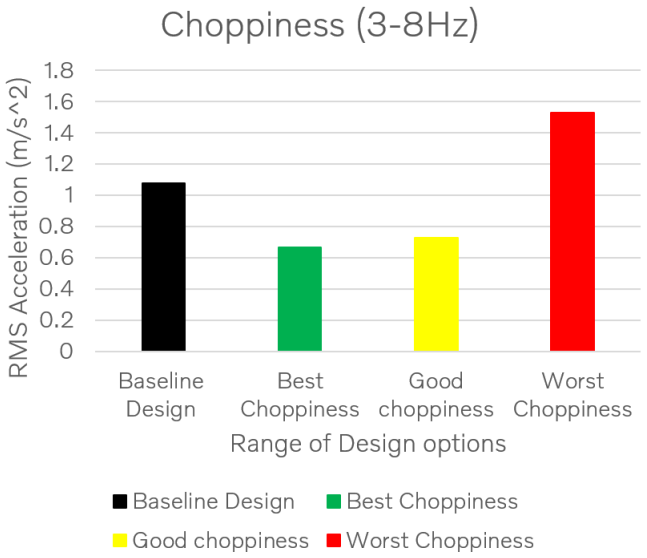

Figure 5.3: Chart indicating the seat RMS acceleration values in choppiness region for chosen design combinations

5.2.2 RMS seat acceleration in shake region with sine wave as road input

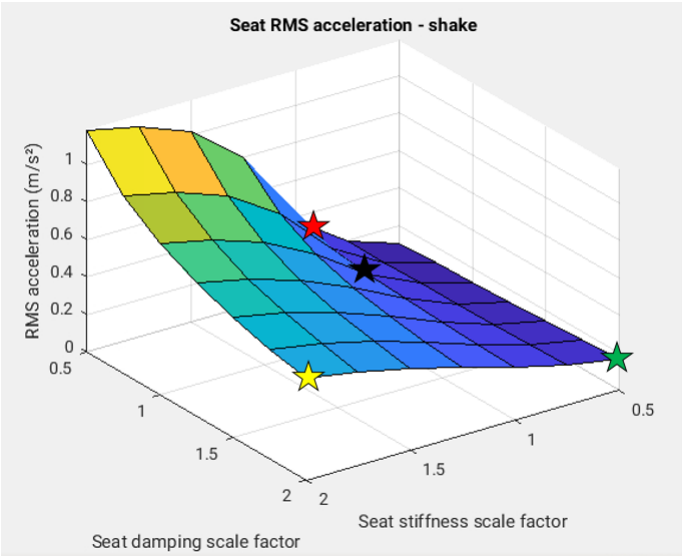

Figure 5.4: 3D surface plot showing the seat RMS acceleration in shake region for various combinations of seat stiffness and damping

Figure 5.4 depicts a 3D surface plot of the seat's RMS acceleration values in the shake region for various combinations of seat stiffness and damping. The green star represents the combination that results in the lowest RMS acceleration value in the shake region, the yellow star represents the value for low shake RMS acceleration value, the black star represents the baseline design, and the red star represents the combination that gives the highest RMS acceleration value in the shake region.

The figure shows that lower seat damping influences RMS acceleration values in the shake region, and the configuration with the highest RMS acceleration value occurs when the seat stiffness is high and the damping is extremely low. In contrast to what was observed in the choppiness region, where stiffer seats resulted in lower RMS acceleration values, we see higher RMS acceleration values in the shake region. In addition, the combination with the lowest seat damping and stiffness has the lowest RMS seat acceleration value in the region of shake, although this combination has a greater RMS acceleration value in the region of choppiness.The combination of high seat damping and low seat stiffness reduces the seat RMS acceleration. This configuration also gives the lowest RMS acceleration value in the choppiness region. Therefore, this would be the ideal configuration of the seat which would reduce the RMS acceleration values in both the choppiness and shake region thereby improving the ride comfort.

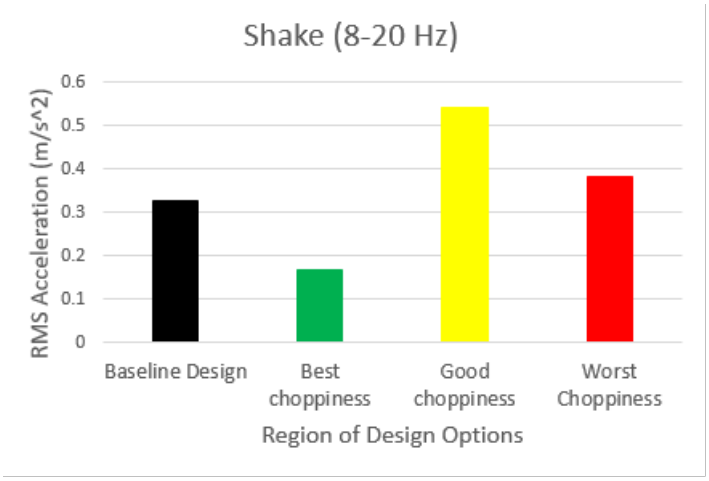

Figure 5.5: Chart indicating the seat RMS acceleration values in shake region for chosen design combinations

5.2.3 RMS seat acceleration in choppiness region with rough road as road input

The rough road as shown in figure 3.15 was given as an input to the model to test whether these combinations give the similar results when a real road is tested. The model was now run by giving the inputs in both the axles. The seat parameters were varied as done for the previous test when sine wave was given as the input. The results from the test showed that the seat RMS acceleration values followed the same trend as observed with the sine wave.

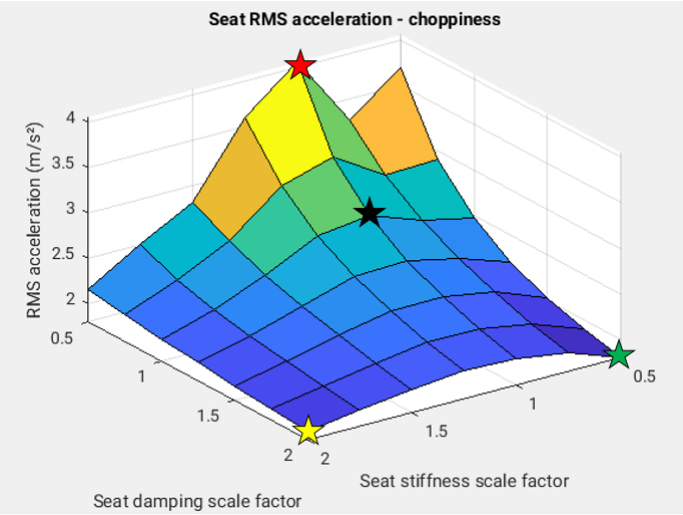

Figure 5.6: 3D surface plot showing the seat RMS acceleration in choppiness region for various combinations of seat stiffness and damping when rough road is given as input

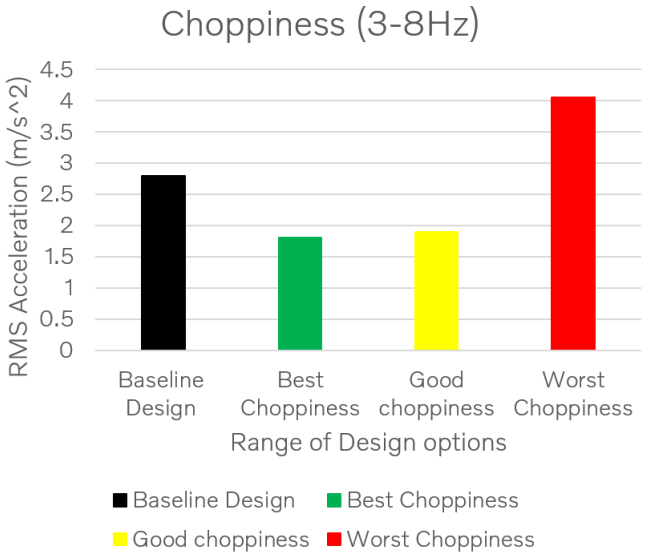

Figure 5.7: Chart indicating the seat RMS acceleration values in choppiness region for chosen design combinations with rough road as input

As shown in the chart above, the magnitude of the seat RMS acceleration is greater when the rough road is used as the input than when the sine wave is used. The same configuration that produced the worst and lowest values of seat RMS acceleration in the choppiness region when a sine wave was used as an input produced the same results when a rough road was used as an input. The trend which indicated that soft seats with more damping reduced the choppiness with the lowest RMS acceleration values followed. The figure 5.6 also showed that lower the seat damping, greater the RMS acceleration values in the choppiness region. Also, when damping is low, the system becomes unstable, resulting in a drop in RMS values followed by a sharp

spike in the region where choppiness is high.

5.2.4 RMS seat acceleration in shake region with rough road as road input

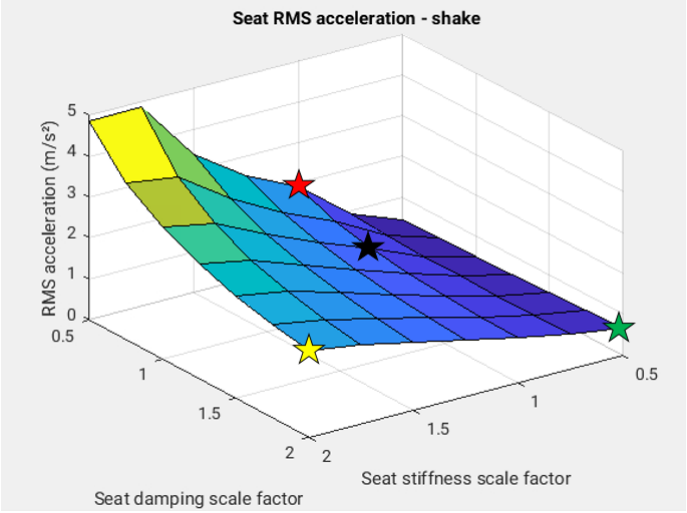

Figure 5.8: 3D surface plot showing the seat RMS acceleration in shake region for various combinations of seat stiffness and damping when rough road is given as input

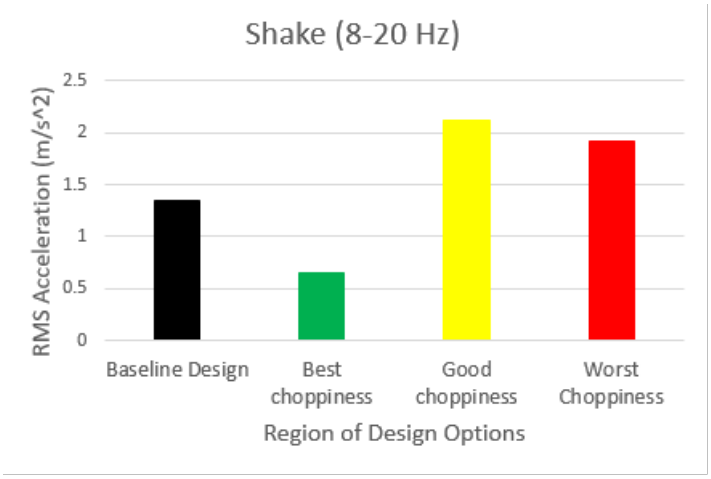

Figure 5.9: Chart indicating the seat RMS acceleration values in shake region for chosen design combinations with rough road as input

The seat RMS acceleration values in the shake region also followed the same trend when the sine wave was given as input. The similar configurations gave the lowest and highest RMS acceleration values. This is depicted by figure 5.8. The figure also shows that stiffer seats indicated higher RMS acceleration values. The configuration with high damping and softer seats was the ideal combination once again as it reduced the RMS acceleration value in the shake region by a considerable margin

from the baseline design's value and also produced the lowest seat RMS acceleration value in the choppiness region. Figure 5.9 shows that magnitude of the seat RMS acceleration values where higher when the sine wave was given as input.

5.3 RMS seat accelerations of ICE ride model

The seat parameters were varied for the ICE ride model when the sine wave was given as the input in the front axle. The varying of seat parameters and studying the effect of it on the seat RMS acceleration values in the choppiness and shake region was primarily done due two reasons; the first being to prove the problem statement of the thesis, which stated that choppiness levels in the ICE vehicle are lower when compared to the BEV, and the second was to compare the trends in seat RMS accelerations between the BEV and ICE vehicles and see if the seat model in the ICE also follows.

5.3.1 RMS seat acceleration in choppiness region with sine wave as road input

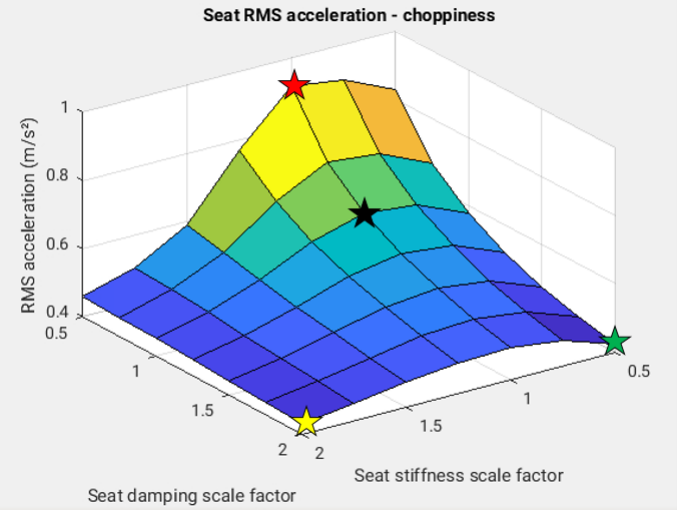

Figure 5.10: 3D surface plot showing the seat RMS acceleration in choppiness region for various combinations of seat stiffness and damping for the ICE ride model

The figure 5.10 indicates that trend in seat RMS acceleration values in the choppiness region is similar to the results of the BEV. Once again stiffer seats reduced the RMS acceleration values thereby decreasing the choppiness. Seat damping also had an effect on the RMS acceleration results, with low damping increasing the values and high damping decreasing the choppiness. The ideal configuration which gave the lowest seat RMS acceleration value thereby reducing the choppiness was when the seat were softer with high damping. It is observed from figure 5.11 that the baseline design of the ICE has a lower RMS acceleration value when compared to the BEV model's baseline design thereby proving the thesis problem statement.

Figure 5.11: Chart indicating the seat RMS acceleration values of the ICE ride model in choppiness region for chosen design combinations

5.3.2 RMS seat acceleration in shake region with sine wave as road input

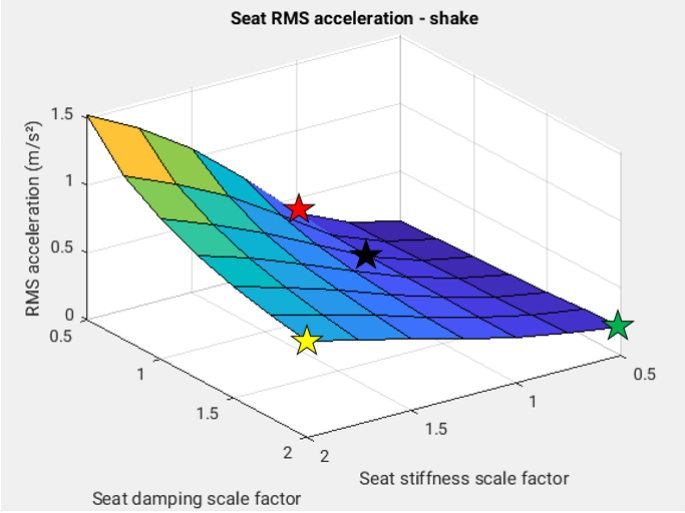

Figure 5.12: 3D surface plot showing the seat RMS acceleration in shake region for various combinations of seat stiffness and damping for the ICE ride model

Figure 5.12 depicts a 3D surface plot of the seat's RMS acceleration values for the ICE ride model in the shake region for various combinations of seat stiffness and damping. From this figure it is observed that the trend in seat RMS acceleration values is similar to that of the BEV's results. The stiffer seats once again resulted in higher RMS acceleration values resulting in large shake. The combination of low seat damping and stiffness results in reducing the RMS acceleration values thereby decreasing the shake. It was also observed that this combination reduced the choppiness level too as indicated in figure 5.10. This configuration was the

optimal design to improve the ride comfort in the BEV as well, therefore indicating that the same approach would improve the ride comfort in the ICE vehicle as well.

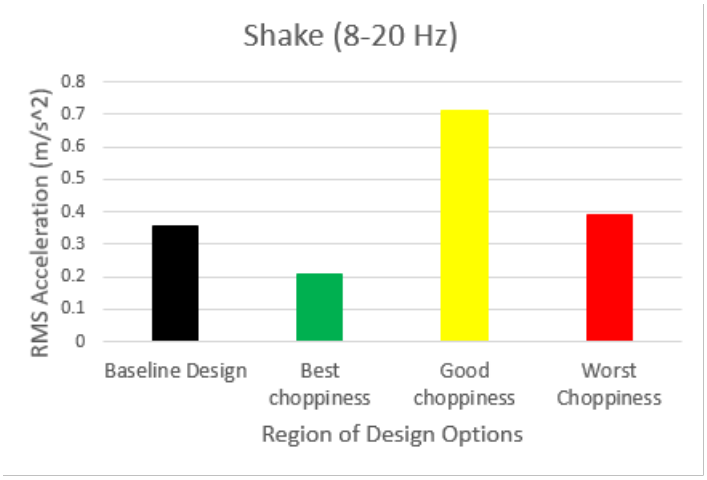

Figure 5.13: Chart indicating the seat RMS acceleration values of the ICE ride model in shake region for chosen design combinations

5.4 Conclusion

As indicated by the results, there is a scope to reduce the perceived vertical choppiness of an electric vehicle by improving the seat parameters. The results show that increasing the seat stiffness and damping reduces choppiness by increasing the rms acceleration values in the shake region, which increases the disturbances felt in the shake region (8-20 Hz). Also, by lowering the seat stiffness and damping values, the RMS acceleration values in the shake region are reduced, reducing the disturbances felt in the shake region; however, this configuration increases the RMS acceleration in the choppiness region, causing the driver to feel more vertical choppiness in the seat. As mentioned previously even though the main objective of the thesis is to reduce the choppiness levels in the seat felt by the driver, it is also important to have a design which performs well in the shake region as well ensuring the overall ride comfort of the vehicle is good. Seats with softer stiffness and high damping characteristics are the optimal solution for reducing RMS acceleration in both choppiness and shake regions and thus providing a comfortable ride.

According to the validation section, a linear CAE ride model was sufficient for an electric vehicle, but a non linear ride model was required for an ICE vehicle to produce results that were comparable to the shake rig tests. The transmissibility plots in the second ride region, particularly in the choppiness region, revealed that when a linear ICE ride model was used, the correlation between the simulink model's results and the shake rig results was poor, whereas when a non linear ICE ride model was used, the correlation was better. Because the ICE vehicle has hyrdo-mounts on which the engine is mounted and these bushings are frequency dependent, the CAE ride model was designed in such a way that non linear dampers and springs that are frequency dependent were modelled as hydro mounts on which the engine

was mounted. Nonlinearity and friction in shock absorbers were also found to be necessary for a better overall correlation. The ride model of a BEV can also be improved by using non linear shock absorbers, resulting in a model that is more realistic. However, the BEV vehicle chosen did not have hydro mounts on which the electric motor was mounted, so a linear model was sufficient to obtain a good correlation between the shake rig and ride model results.

6 Future Scope

The thesis's scope was limited to identifying the possibility of using the seat to reduce perceived vertical choppiness. The thesis findings indicate that by adjusting the seat parameters, such as seat stiffness and damping, the perceived vertical choppiness can be reduced. To put the thesis findings into practice in the future, the main task would be to collaborate closely with the seat and ergonomics departments to gain a better understanding of seat stiffness and damping and, as a result, determine the most optimal seat design to reduce choppiness. Because modeling humans as spring mass damper systems is a difficult task, it is necessary to improve the design of the human and seat models in order to gain a better understanding of choppiness effects in humans. Furthermore, the work done thus far has primarily focused on a linear ride model, despite the fact that real systems are far from linear. As a result, the CAE ride models must be improved by taking nonlinearity into account. This can be done by considering friction in the dampers, making the shock absorbers and bushings nonlinear, and thereby designing models that are close to reality.

Bibliography

[1] X. Wang, A-L. Osvalder, P. Höstmad, and I. Johansson (2020). “Human Response to Vibrations and Its Contribution to the Overall Ride Comfort in Automotive Vehicles: A Literature Review”, SAE Technical Paper, 2020.

[2] X. Wang, A-L. Osvalder and P. Höstmad (2022). “Noise and Vibration Influence on Overall Ride Comfort in a Conventional Passenger Car under Different Driving Scenarios”. To be submitted for publication.

[3] X. Wang, P. Höstmad and A-L. Osvalder (2022). “Influence of Sound and Vibration on Perceived Overall Ride Comfort: Comparison between an Electrical Vehicle and a Combustion Engine Vehicle”. To be submitted for publication.

[4] Hanumantha Gowda, Hemanth and Smith, Joshua (2022).Objective Seat Comfort Assessment using Finite Element Human Body Model Simulations. Chalmers ODR. https://odr.chalmers.se/items/dba90cab-b900-4d38-85ec-3db49e97e374

[5] Kuijt-Evers, d., deLooze, M. P. Dieen , V. J., 2003. Sitting comfort and. Ergonomics, Volume 46, No. 10, pp. 985-997.

[6] Ö. Gündoğdu," Optimal seat and suspension design for a quarter car with driver model using genetic algorithms ". https://doi.org/10.1016/j.ergon.2006.11.005

[7] Martin G.R. Toward, Michael J. Griffin." The transmission of vertical vibration through seats: influence of the characteristics of the human body". https://doi.org/10.1016/j.jsv.2011.07.033

[8] Jin L, Yu Y, Fu Y. Study on the ride comfort of vehicles driven by in-wheel motors. Advances in Mechanical Engineering. 2016;8(3). https://doi:10.1177/1687814016633622

[9] Abbas, W. , Emam, A. , Badran, S. , Shebl, M. and Abouelatta, O. (2013) Optimal Seat and Suspension Design for a Half-Car with Driver Model Using Genetic Algorithm. Intelligent Control and Automation, 4, 199-205. doi: 10.4236/ica.2013.42024.

[10] Jacobson, Bengt (2022). "Vehicle Motion Engineering Compendium " .

[11] Gillispie, Thomas(1992). "Fundamentals of Vehicle Dynamics" .

[12] J.Y.Wong (2001)."Theory of Ground Vehicles(3rd ed.)" .

[13] S.Rao, Singiresu (2011). "Mechanical Vibrations (5th ed.)".

[14] ISO 2631 Standards,Guide for the evaluation of human exposure to whole-body vibration.

[15] R.Jazar(2008), "Vehicle Dynamics:theory and application".